THE UNIVERSITY OF MICHIGAN

COLLEGE OF ENGINEERING
Department of Meteorology and Oceanography

Part II

VISUAL RESOLUTION AND OPTICAL SCINTILLATION OVER SNOW, ICE, AND FROZEN GROUND

Donald J. Portman
Professor of Meteorology

Edward Ryznar
Research Associate

Floyd C Elder
Associate Research Meteorologist

ORA Project 03372

under contract with:

U. S. ARMY COLD REGIONS RESEARCH AND ENGINEERING LABORATORY
CORPS OF ENGINEERS
HANOVER, NEW HAMPSHIRE
CONTRACT NO. DA-11-190-ENG-78

administered through:

OFFICE OF RESEARCH ADMINISTRATION ANN ARBOR

February 1964

PREFACE

The work described in this report was conducted under U. S. Army Cold Regions Research and Engineering Laboratory, Contract No. DA 11 190 ENG-78. The general purpose of the investigation was to determine and describe the dependence of visual resolution and optical scintillation on meteorological conditions in horizontal optical paths over snow, ice, and frozen ground. Specifically, the work included (1) measurement of resolution, optical scintillation, and micrometeorological variables over snow, ice, and frozen ground, and (2) processing and analysis of the data obtained. The present report includes results of the measurement and analysis programs, a description of equipment used and a discussion of measurement and data processing procedures. It supplements CRREL Research Report No. 111, Part I, "Visual Resolution and Optical Scintillation over Snow, Ice and Frozen Ground" by D. J. Portman, E. Ryznar, F. C. Elder, and V. E. Noble.

The authors wish to express their appreciation to Dr. Vincent E. Noble, Mr. Francis J. Yockey, and Mr. John E. Casey for their assistance in the measurement and analysis phases of the investigation, to Mr. James Kroth and (Mrs.) Ruth Baehr for their work in data processing and to (Mrs.) Joy Beil for her efficient preparation of the typescript.

TABLE OF CONTENTS

TABLE OF CONTENTS (Continued)

LIST OF TABLES

LIST OF FIGURES

LIST OF FIGURES (Continued)

LIST OF FIGURES (Continued)

ABSTRACT

The effects of turbulent fluctuations of atmospheric density are seen as rapid changes in the brightness of a distant light source, (scintillation) and in the apparent position, size, and shape of distant objects (shimmer). An investigation of these effects in horizontal optical paths was conducted by measuring visual resolution, optical scintillation intensity and frequency, and wind and temperature profiles over snow, ice and ground surfaces. The data obtained over the various surfaces were analyzed to determine relationships between (1) visual resolution and meteorological conditions and (2) scintillation (intensity and frequency) and meteorological and surface conditions.

Principal results of the analysis of the resolution data obtained over snow and frozen ground showed that for turbulent flow in stable stratification, visual resolution (1) deteriorated systematically as the vertical temperature gradient increased, (2) deteriorated with clear skies as the wind speed increased up to about 5 mph and then improved at higher wind speeds, and (3) was optimum and nearly independent of wind speed during low overcast cloudiness. Over a snow-free ice surface and with air temperatures below freezing, only minor scintillation was observed. Resolution conditions were excellent during wind speed and sky conditions normally conducive to higher scintillation intensity and poorer resolution over ground or snow-covered ground. As the snow depth on the ice increased, the behavior of scintillation intensity approached that observed over ground and snow covered ground. The scintillation data obtained over ice are interpreted with regard to wind and temperature structure above the ice and to the heat conducted upward through the ice.

A photographic method to measure resolution is described and some results are presented. Power spectra of scintillation over different surfaces are shown and discussed in relation to various meteorological parameters.

These and other relationships are discussed and equipment and measurement procedures are described.

1. INTRODUCTION

1.1 The Problem

When an observer tries to see a distant object through a clear atmosphere his ability to discern the object clearly may be influenced by several phenomena. According to Wimbush (1961), these are:

1. Scintillation, which is defined as apparent fluctuations in intensity of light from the object. The overall effect is referred to as brightness scintillation and the intensity of fluctuations at different wave lengths is called color scintillation. Each may be observed with the naked eye in the twinkling of stars.
2. Oscillating object motion, which may be classified as apparent wandering or dancing, according to its frequency.
3. Object enlargement, which consists of slow apparent fluctuations of object size at frequencies roughly corresponding to those of wandering (focus drift) or faster fluctuations having frequencies which approximate those of dancing (pulsations). There may also be a steady blurring (tremor disc) of the object.

For either visual or photographic observation, the seeing phenomena which are most injurious to object resolution are dancing, pulsation, and tremor disc. Their combined effect is called boil or shimmer. The visible effect is an apparent smearing of the object and a reduction of contrast both within the object and between the object and its background. Because these phenomena are most pronounced in clear weather when visual resolution otherwise would be unimpeded, they act as the limiting factors in the ultimate resolution obtainable with optical devices for distant viewing.

Shimmer and scintillation are caused by small-scale variations in atmospheric density associated with incomplete turbulent mixing of thermally stratified layers. They are absent in isothermal conditions and have a maximum intensity, dependent upon wind and surface roughness conditions, for maximum vertical temperature gradients. The dependence of scintillation and shimmer on meteorological conditions near the ground suggests that if quantitative relationships were known, it would be possible to predict the deterioration in visual resolution from meteorological and surface data for any time and region of concern.

1.2 Previous Work

Work for the U. S. Army Cold Regions Research and Engineering Laboratory (then SIPRE) on scintillation and visual resolution problems was begun by University of Michigan personnel in early 1960. The first field experiments were conducted over snow at the CRREL Keweenaw Field Station (henceforth abbreviated as KFS), Houghton, Michigan in February and March, 1960. In 1961, limited data were also obtained over ice and frozen ground, respectively, at Ford Lake near Ypsilanti, Michigan, and at Willow Run Airport, Michigan.

The information obtained over snow enabled studies to be made of (1) the intensity and frequency characteristics of optical scintillation in relation to atmospheric turbulence and (2) visual resolution in relation to scintillation characteristics.

1.3 Papers and Reports

The work up to June, 1961, was presented in CRREL Research Report No. 111, Part I entitled "Visual Resolution and Optical Scintillation over Snow, Ice, and Frozen Ground" by D. J. Portman, E. Ryznar, F. C. Elder, and V. E. Noble.

Two papers were presented at the 203rd National Meeting of the American Meteorological Society held at the University of Alaska in June, 1962. They were "Some optical properties of atmospheric turbulence" by F. C. Elder, D. J. Portman and V. E. Noble, and "Scintillation and visual resolution over snow" by E. Ryznar and F. C. Elder.

Early results of the work were described in a paper entitled "Some optical properties of turbulence in stratified flow near the ground," by D. J. Portman, F. C. Elder, E. Ryznar, and V. E. Noble published in the Journal of Geophysical Research, July, 1962, and in the Proceedings of the IUGG-IUTAM on Turbulence in Geophysics, Marseilles, France, September, 1962.

Results of the analysis of the visual resolution data are discussed in the article "Visual resolution and optical scintillation in stable stratification over snow" by E. Ryznar, published in the August 1963 issue of the Journal of Applied Meteorology.

2. VISUAL RESOLUTION OVER SNOW

2.1 Introduction

The general approach to the ultimate goal of predicting visual resolution from meteorological and surface information was presented in Fig. 1, Part I. It was based on the idea that the limiting factors in the resolution obtainable with optical devices for viewing a distant object in a clear atmosphere were shimmer, or apparent object motion, and scintillation, or apparent brightness fluctuation of the object. Since both phenomena are caused by fluctuations in atmospheric density associated with turbulence in the line of sight, it was reasoned that shimmer and scintillation (for a given path length and height) would be uniquely determined by the degree of stratification and the characteristics of turbulence. Over level and uniform terrain they would depend, therefore, on the mean vertical temperature gradient, wind speed and direction (relative to the line of sight) and surface roughness.

Of major importance to the realistic application of the field results to practical problems, however, is the fact that the detailed measurements of vertical temperature gradients are not routinely available. In order to apply the results in this sense, therefore, it is necessary to rely upon general knowledge of the occurrence of different combinations of wind and temperature conditions near the ground for a wide variety of meteorological situations. Since a given wind and temperature regime near the ground may be established by any one of a large number of different combinations of external atmospheric conditions, it is impractical to seek valid general relationships between visual resolution and scintillation and the latter conditions. The vertical temperature gradient serves as an intermediate step in the prediction scheme; it must be estimated or predicted from such information as cloudiness, time of year, surface conditions, wind speed, etc.

Much of the analysis of Part I consisted of formulating relationships of scintillation intensity (P_m) as observed in stable stratification over snow to inversion magnitude, wind speed and Richardson number. A relationship of visual resolution to scintillation was also established.

The following two sub-sections contain material continuing the analysis of the same data. In the first section it is shown that, like scintillation, visual resolution bears a close relationship to the mean thermal stratification. The analysis in the second section shows that, for the conditions of the experiments, visual resolution could be estimated directly from knowledge of cloudiness and wind speed. The difficulty of generalizing from such relationships is illustrated in the third section. Here, in a detailed study of a special case, it is shown that the advection of cold air at night prevented the formation of thermal stratification with a clear sky and light wind. The

analyses emphasize the necessity of relating visual resolution to characteristic flow parameters for general practical use.

2.2 Results and Discussion

2.2.1 Resolution and Vertical Temperature Gradient -- In Part I, a relationship between P_m and inversion magnitude over snow was discussed. It showed a systematic increase of P_m with increasing temperature difference between 50 and 400 cm above snow. Since P_m is a measure of scintillation intensity and shimmer and since it has been established that the intensity of shimmer determines resolution conditions, it follows that resolution should also be determined by the vertical temperature gradient. The dependence of the smallest discernible slot sizes on the temperature difference between 50 and 400 cm above snow is shown in Fig. 1 for a total of 126 observations obtained at night. Each point is the average of the resolution observations within successive one-degree temperature differences. The number of observations is indicated below each point. The dashed curve is a visual estimate of the best fit curve.

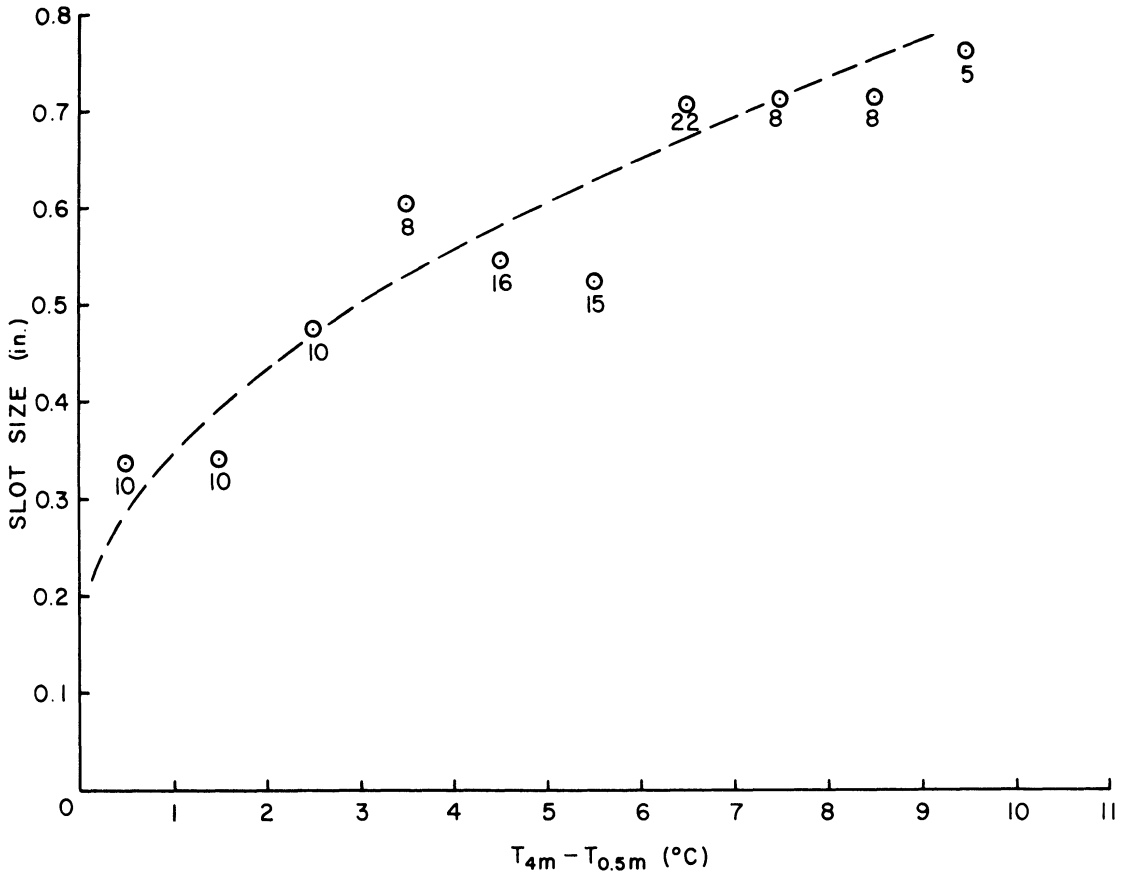

Figure 1. Smallest Discernible Slot Size vs. Temperature Difference Between 4 and 0.5 Meters at Night over Snow

A systematic deterioration of resolution with increasing inversion magnitude is evident. At temperature differences less than 1°C the orientations of slot sizes which averaged about 0.34 inch could be detected, but for differences between 9 and 10 C the average smallest, discernible slot size increased to about 0.76 inch. The data were not categorized according to turbulence characteristics, pressure, cloudiness, or absolute temperature, so each point represents an average for a large range of these conditions.

2.2.2 Resolution and Wind and Cloudiness -- Because cloudiness and wind speed exert a pronounced influence on the temperature profile, the same resolution limit data were categorized according to the amount of cloudiness and related to wind speed. The value of these parameters is that they are readily available from standard weather station observations in contrast to the temperature profile which requires detailed measurements. The results obtained over snow at night are shown in Fig. 2. Relationships of resolution to the 2 meter wind speed are shown for two general sky conditions: (1) clear or scattered and (2) broken or overcast. The number of observations is indicated below each point. The dashed curve is a visual estimate of the best fit curve.

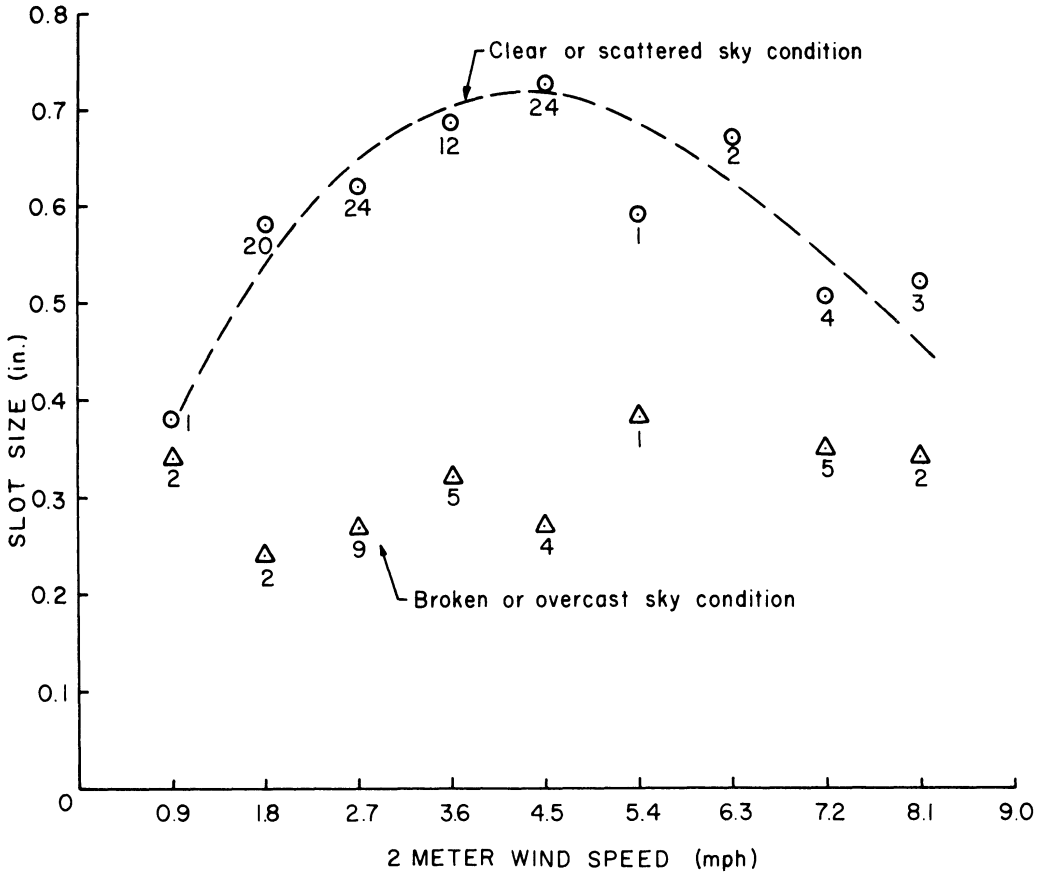

Figure 2. Smallest Discernible Slot Size vs. Wind Speed at 2 Meters at Night over Snow for (1) Clear or Scattered Sky Condition and (2) Broken or Overcast Sky Condition

For a clear or scattered sky condition, the deterioration in resolution is evident by the increase in the smallest discernible slot size from an average of 0.38 to 0.72 inch as the wind speed increases to about 5.0 mph. It may be reasoned that an increase in wind speed from nearly calm to about 3-5 mph caused vertical motions to increase because of wind shear effects. The magnitude of temperature fluctuations increased correspondingly, shimmer increased, and resolution deteriorated. However, the same wind shear effects above this speed tended to decrease the temperature gradient through mixing action, even though vertical motions continue to increase. As a result, the magnitude of temperature fluctuations decreased, shimmer decreased, and the improvement in resolution is evident by the decrease in the smallest discernible slot size from an average of 0.72 to 0.5 inch. Presumably, resolution would continue to improve as wind speed increased until the absolute limit of the observer and telescope system (about 0.2 inches for the 543 m optical path) were reached.

For broken or overcast sky conditions, indicated by triangular points, fewer observations were available, but resolution in all such cases was much better and nearly independent of wind speed. The average discernible slot size for these conditions was 0.3 inch. Such behavior reflects the smaller initial temperature gradients with these sky conditions. Although vertical motions increased with wind speed, the magnitude of temperature fluctuations remained small, shimmer remained low, and resolution remained quite good.

The relatively few observations of resolution made over snow in daytime correspond in a general way with those obtained at night. However, average resolution conditions were much better in daytime than at night. Such conditions would be expected from the fact that all vertical temperature differences measured for the daytime observation periods were relatively small.

2.2.3 Advection Effects on Resolution -- The observations on which both relationships in Fig. 2 are based were obtained at subfreezing temperatures and during nocturnal inversions which formed due to net radiation losses from the snow surface. As a result, the general validity of these relationships and the statements regarding daytime resolution is limited by possible advection effects. For example, the advection of extremely colder air on a clear night can conceivably inhibit shimmer by suppressing inversion formation. Such a condition was experienced on the night of 1 March 1962 at the Willow Run Field Station.

A section of the surface weather map for the area of interest near the time of field observations (2100-2200 EST) is shown in Fig. 3. The field station is indicated by the letters YIP near Detroit. Isobars are drawn for every millibar of sea level pressure. Temperatures, dew points and wind velocities are given for selected stations. The map shows an intense, cold high-pressure area centered in the north-central part of Lower Michigan with temperatures of -18 and -19F in the northwest part of the state and about +5F

at Willow Run. The clockwise circulation around the high pressure center caused a continuous influx of colder air at Willow Run with northeasterly winds of about 3 mph. The sky was clear and the ground was frozen and covered by hardpacked snow about 8 cm deep.

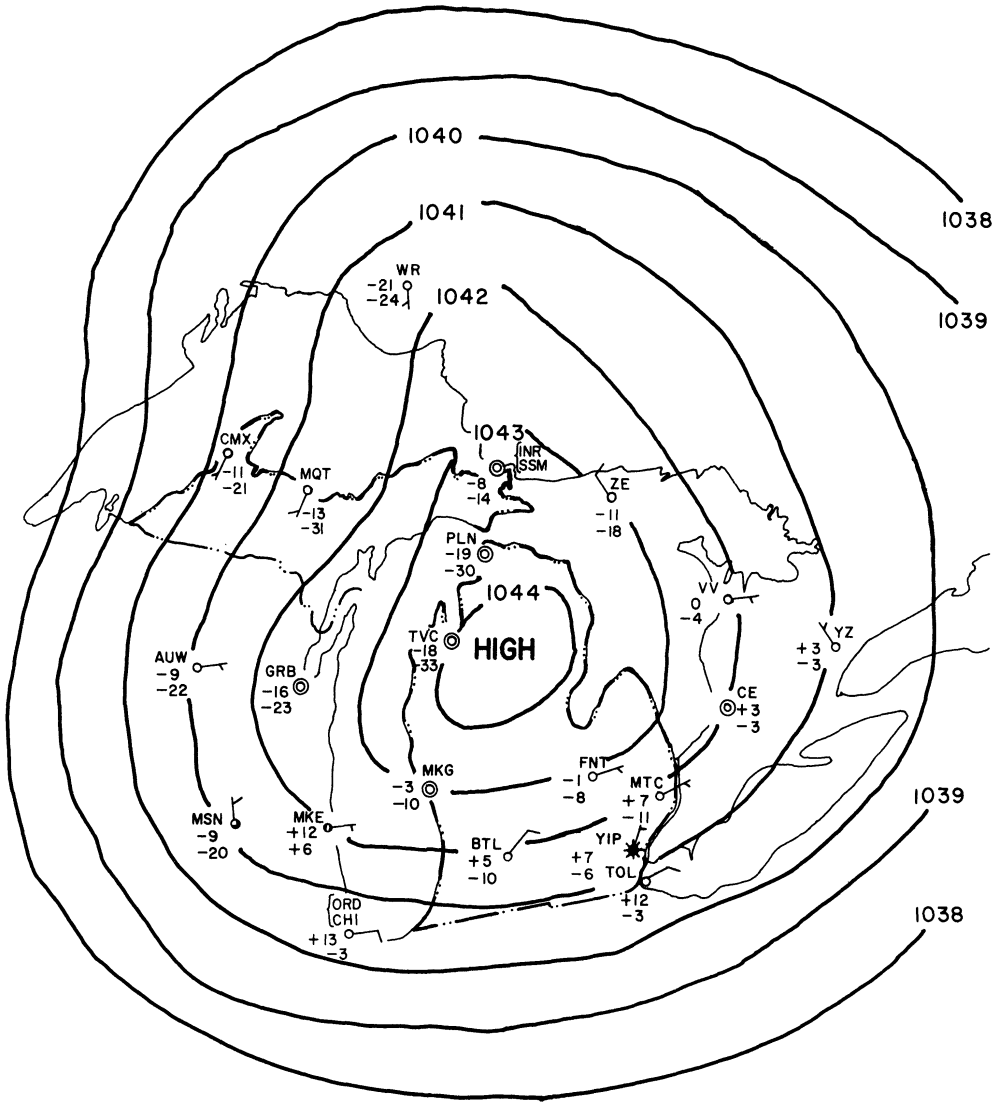

Figure 3. Surface Weather Map for 2200 EST, 1 March 1962

With such sky, wind, and surface conditions, a strong inversion, high scintillation and generally poor resolution would have been expected (Fig. 2). Instead, however, scintillation was low, resolution was good, and an average temperature lapse of about -0.2C between 50 and 400 cm was measured. The wind speed itself was not thought to be high enough to destroy the inversion. The continuous influx of colder air was apparently balancing the net radiation losses from the snow surface despite the prevalence of clear skies because neither the air temperature nor the temperature profile changed appreciably

in the 3 hour observation period. Although such a condition is infrequent as evidenced by the fact that this was the only obvious occurrence in the entire series of field experiments, it does represent an anomaly that could be more frequent at other locations.

In addition to the effects of cold air advection on resolution, the advection of air which is well above freezing could also produce resolution conditions which would not be predicted by a relationship of resolution to wind speed - cloudiness such as that shown in Fig. 2. In this case, an advection inversion would result. Intense shimmer and poor resolution could presumably exist at quite high wind speeds and would be nearly independent of sky condition or time of day. Field experiments were not conducted under such conditions but the occurrence could be quite common in the spring season if a melting snow or ice cover still existed when daytime temperatures were well above freezing.

3. PHOTOGRAPHIC RESOLUTION

3.1 Introduction

As discussed in Part I, the Landolt Ring chart provided significant results regarding visual resolution for different scintillation and meteorological conditions. There were, however, several disadvantages in its use in the field experiments. Among these were the following: (1) Several minutes were required to determine the limit of resolution. This disadvantage was most noticeable during conditions of large inversions and low wind speeds, when the level of shimmer was very high and also extremely variable. Observations of visual resolution in such cases could not often keep up with the rapid changes in shimmer, so that the accepted resolution limit did not always correspond to a coincident measurement of Pm. (2) The psycho-physical condition of the chart observer played an important though unevaluated part in the observations. (3) During periods of low temperature, occasional delays in a series of observations of resolution occurred because moisture condensed on the eyepiece of the telescope used to view the chart. (4) To obtain resolution observations in the field required two people; one to manipulate the chart and one to observe it, so that monitoring the operation of other equipment was interrupted unless additional manpower was available.

Because of these disadvantages a photographic method was designed for use in the 1962 field experiments. Instead of an observer viewing the chart, a camera and lens system was used, and instead of the Landolt Ring chart as a target, an improved resolution chart was constructed and used.

3.2 Equipment and Procedures

3.2.1 Bar Resolution Chart -- Fig. 4 shows the resolution chart mounted in the shelter as it was used in the field. Its design is based on a National Bureau of Standards high contrast resolution chart and its specifications are given in Table I. The chart consisted of two sets of fourteen groups of bars, one set of which was positioned at one-half meter and the other at one meter above ground. Each group in each set consisted of three vertical, black bars reproduced photographically and dry-mounted on a 4' x 5 1/2' section of white masonite. The widths of the bars within each group were equal and ranged from 3.04 cm within the largest group to 0.15 cm in the smallest. The bar width of each successive group was 1.26 times that of the previous group. From a distance of about 300 m, the angular separation of bar widths within each of the fourteen groups varied from 5.0 microradians for the smallest group to 100 microradians for the largest. The groups were numbered consecutively in the order of decreasing bar width and angular separation.

In the field experiments the chart was housed in a small shelter (located near the photometer) to shield it from as much illumination by the

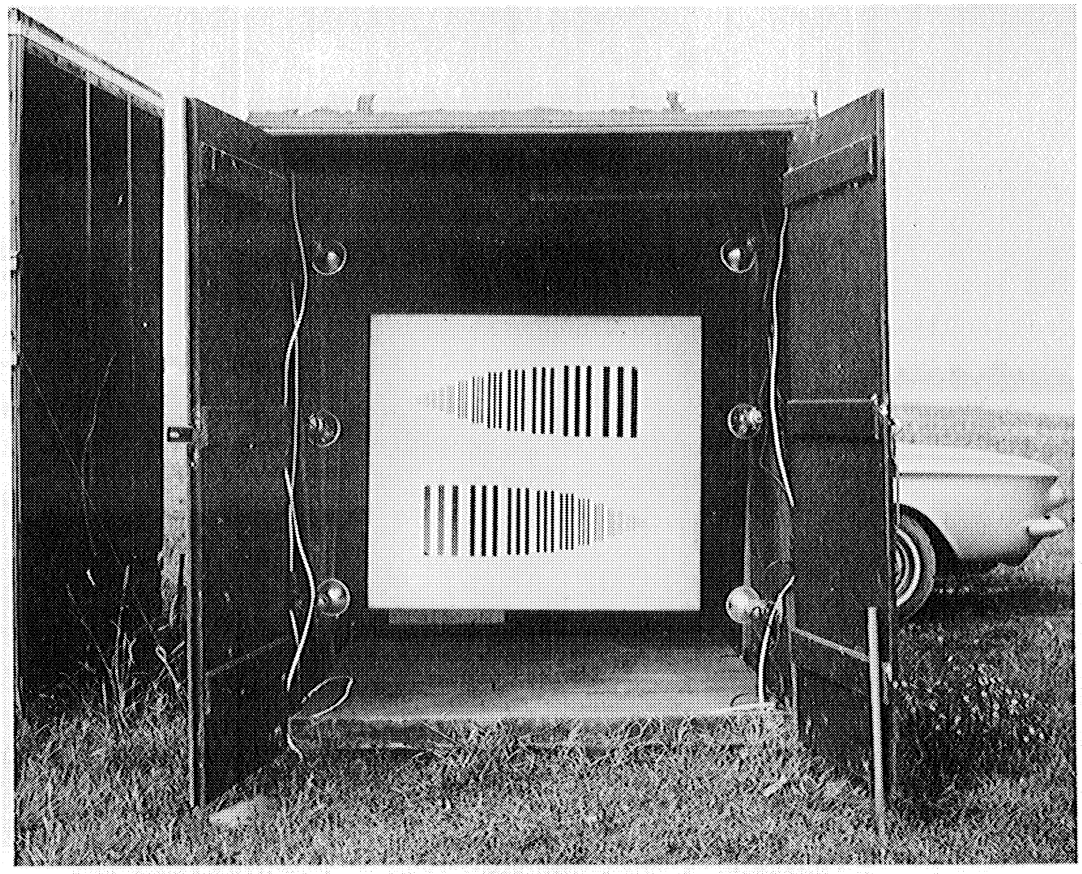

Figure 4. Line Resolution Chart

Table I

RESOLUTION CHART SPECIFICATIONS

Bar Group No.	Bar Spacing cm	Angular Spacing Microradians (300 m Distance)
1	3.04	100
2	2.40	79.2
3	1.92	63.0
4	1.52	50.0
5	1.20	39.7
6	0.96	31.6
7	0.76	25.1
8	0.60	20.0
9	0.48	15.9
10	0.38	12.6
11	0.30	10.0
12	0.24	7.9
13	0.19	6.3
14	0.15	5.0

sun as possible. Also, to minimize any variation in its illumination from day to night, the chart was uniformly illuminated by seven photo flood lights spaced along the walls and floor of the shelter.

3.2.2 Camera, Lens and Film -- The resolution chart was photographed with a Yashica Pentomatic 35mm, single lens, reflex camera from which the lens was removed. The camera was attached to a Kodak Aero-Ektor 610mm f:6.0 lens. Both are shown in Fig. 5. In the field experiments, the camera was focused on the chart with the aid of a ground-glass view finder during minimum scintillation conditions. It was located at a height of one meter and a distance of 300 m from the resolution chart.

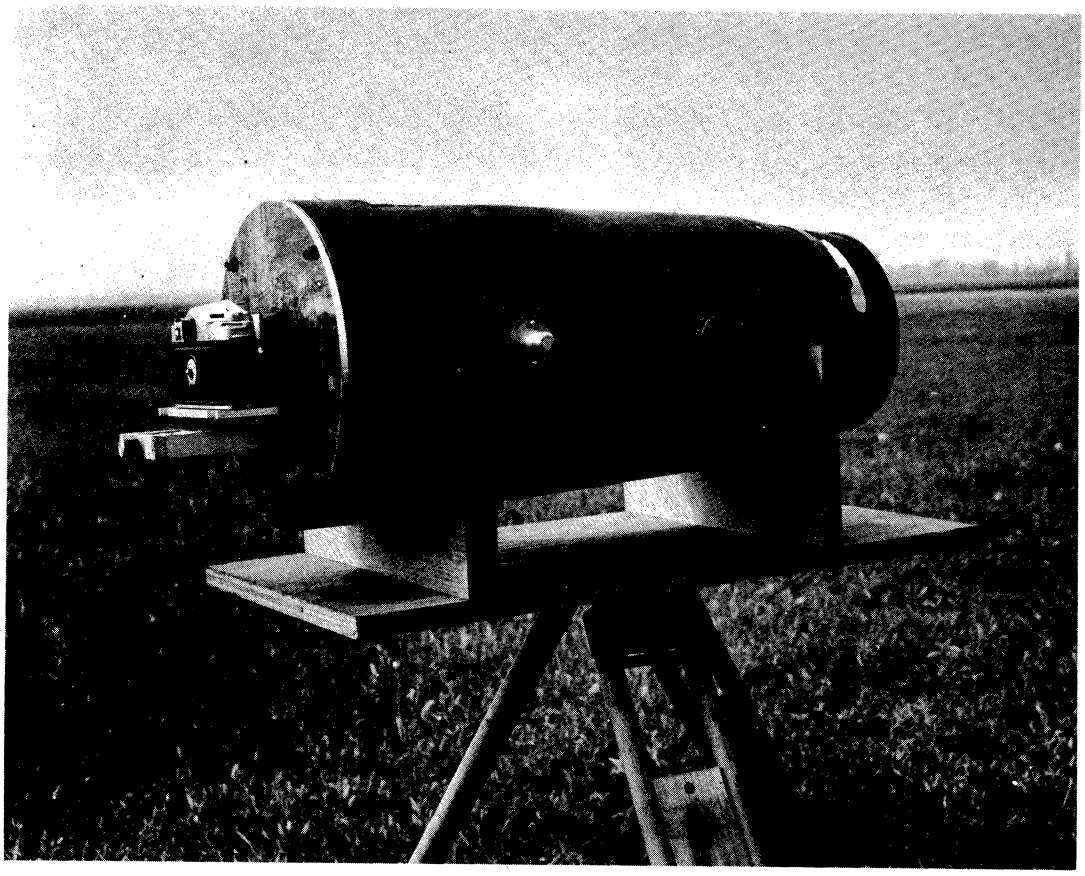

Figure 5. Photographic Resolution System

Theoretically, the composite lens, camera, and film system should give a resolution R equal to

$$R = \left| \left(\frac{1.22\lambda}{D} \right)^2 + \left(\frac{1}{R_F \, D \, (2500 \, t)^{1/2}} \right)^2 \right|^{1/2} \quad \text{radians}$$

where λ is the wave length of light, D is the diameter of the lens, R_F is the resolution of the film, and t is the length of time of the exposure (Boston University, 1957). For the present system:

$$\lambda = 0.57 \times 10^{-4} \text{ cm}$$
$$D = 10.16 \text{ cm}$$
$$R_F = 1000 \text{ lines/cm}$$
$$t = 0.001 \text{ seconds}$$

so that

$$R = \frac{4836}{D^2} + \frac{39.36}{D^2 t} = 20.69 \text{ microradians}$$

To test the system, photographs of an NBS high-contrast resolution test chart were taken over an undisturbed laboratory test path of 40 feet. The results of the tests showed that the camera-lens system had an angular resolution limit of approximately 35 microradians. For use with the resolution chart in the field experiments, the system, therefore, could not be expected to resolve any bar group smaller than the sixth, which had a bar spacing of 0.96 cm and corresponded to an angular separation of about 32 microradians when photographed from 300 m. Thus, even under the most ideal seeing conditions, the resolution limit could not be expected to be better than group six.

Kodak Plus-X film was used almost exclusively during the field experiments because of its moderately fine grain size and its fast speed. With Plus-X film, an exposure of 1/1000 second at f/6 produced the most satisfactory photographs. Also, the clearest photographs resulted when the film was developed in Acufine film developer at full strength for 4 1/2 minutes at 20C. The resulting film strip contained negatives of the resolution photographs. Each photograph had dimensions of 2 x 3 mm and showed the sets of bars at both heights.

3.2.3 Resolution Determination -- One method to evaluate resolution photographs was to place the film strip on a light table and visually to scan each photograph through a 12 power hand magnifier. Since the effect of shimmer was to fuse the black bars into the white background, the resolution limit of each photograph became the angular resolution of the smallest group within which the separation of individual bars was still distinct.

A second method consisted of the use of a densitometer to scan the chart photographs. Briefly, the device consisted of a light source to illuminate the negative, a series of condensing lenses, a pinhole on which the light passing through the negative was focused, a photocell which received the light passing through the pinhole, and a recorder for the photocell output. As the device scanned across each group on a chart photograph, the recorded

output of the photocell varied with the amount of light passing through the pinhole.

A typical recorder trace is shown in Fig. 6. The trace consists of a series of three peaks and two valleys whose sharpness depends on the distinctness of the three bars comprising each group on the chart. Since a negative is being scanned, a crest represents a bar on the chart and a trough represents a white space. As the trace is followed from right to left and a group is approached which represents the resolution limit for a certain shimmer condition, the device sees progressively less contrast between the bars and the background and the amplitudes of the crests and troughs on the recorder trace decrease. For this particular trace, the fifth group became the resolution limit and corresponded to an angular separation of 39.7 microradians.

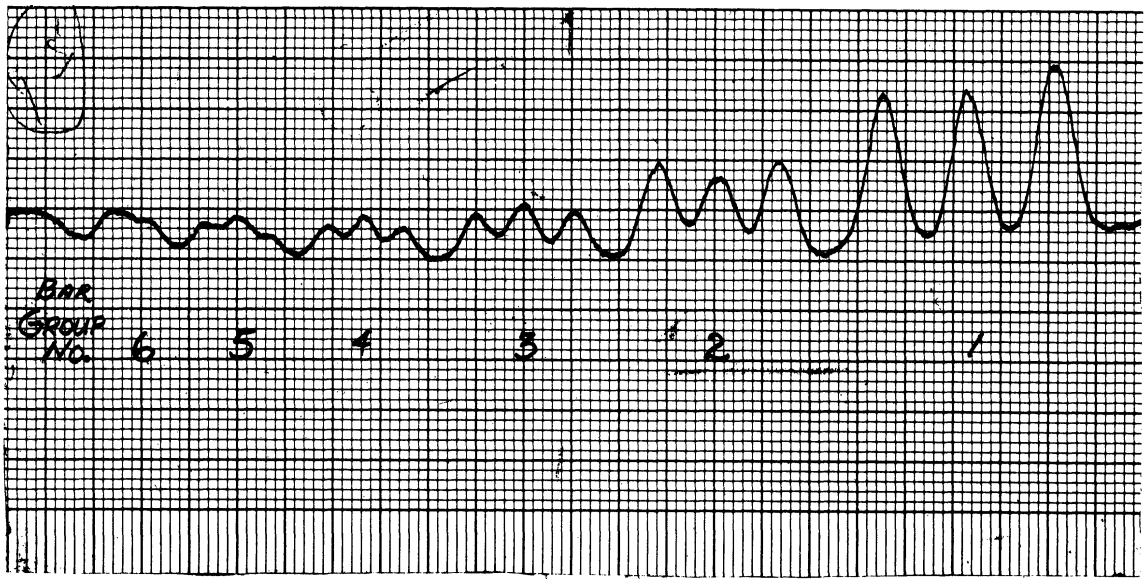

Figure 6. Densitometer Trace for 1942 EST, 3 April 1962

Two disadvantages of the method were soon apparent. (1) The decision required to evaluate the recorder trace in terms of a resolution limit was usually as difficult to make as that involved in field observations with the Landolt Ring chart, and (2) The densitometer scanned only a finite section of each bar length. Regarding the second disadvantage, there were cases when all other sections of the bars were distinct except for the small section

which was scanned by the densitometer because it was blurred either by shimmer or by a film irregularity. An unreal resolution limit resulted. Because of these disadvantages the photographs were evaluated by means of the visual method. Although a decision still had to be made concerning the resolution limit, it was felt that a more accurate one could be made by scrutinizing visually the entire chart photograph than by evaluating a recorder trace which represented only a narrow path through the chart. The same observer evaluated all photographs. In his judgment, if he were certain of the resolution limit, the exact bar group number was noted. However, if the resolution limit was determined to be slightly better or worse than a given bar group number, the group number was labeled plus or minus, respectively.

3.3 Results and Discussion: Photographic Resolution and Scintillation

Approximately 48 resolution photographs were taken over a 300 m path at the Willow Run Field Station during both temperature lapse and inversion conditions. Fig. 7 shows the results of relating the resolution limit of 33 photographs of the chart at one meter to P_m. (See Section 4.2.2 for a discussion of scintillation recording equipment changes and their effects on P_m). More precisely, the angular resolution of the resolution limit group is related to P_m. The points are averages of P_m values for each bar group and the number of observations is indicated below each point. The points between the group numbers resulted by assigning plus or minus to certain resolution limits in the process of interpreting the photographs, as discussed previously.

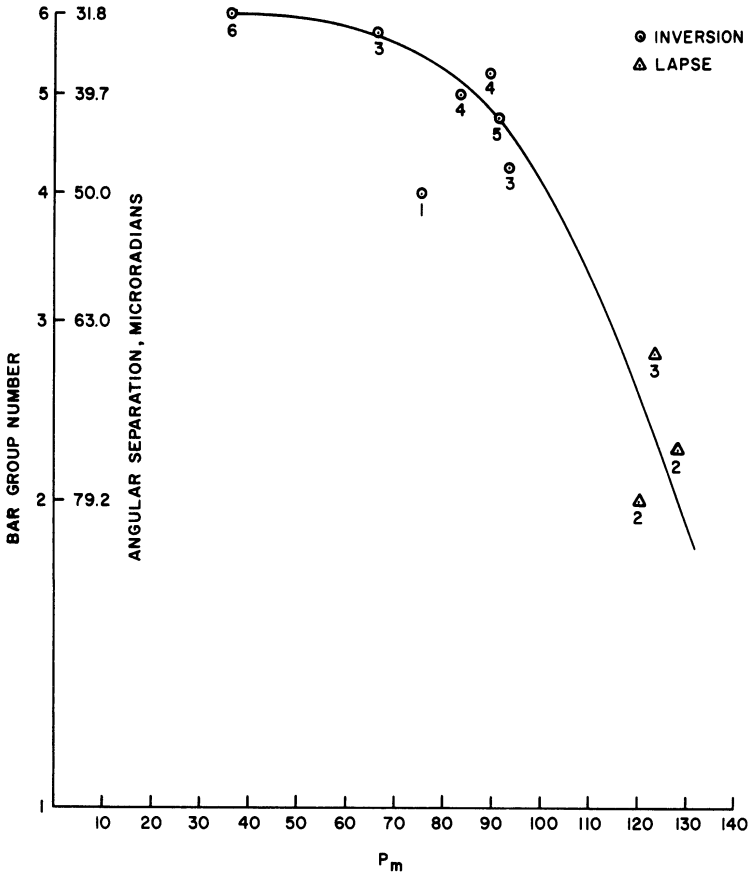

Figure 7. Angular Separation of Resolution Groups vs. Per Cent Modulation for Lapse (▲) and Inversion (⊙) Conditions

A decrease in photo resolution (P.R.) with increasing P_m is evident. Average values range from the low shimmer and good resolution observation of $\overline{P_m}$ = 36, P.R. = 31.8 microradians (group No. 6) to the high shimmer and poor resolution observation of $\overline{P_m}$ = 120, P.R. = 79.2 microradians (group No. 2). The first average also includes some resolution data obtained during adiabatic temperature profile conditions when the resolution was optimum. Such photographs represent the limit of resolution capability of the system which was shown previously to be group No. 6. The result is that as long as the same lens system is used to photograph the chart and the distance between the chart and camera remains constant, any curve relating resolution to P_m must end at that group. If a more powerful lens had been available, a larger group number (smaller size) would have been resolvable during ideal seeing conditions. In addition, a greater number of intermediate group could be used to represent intermediate seeing conditions.

3.4 General Conclusions

The photographic method of obtaining resolution measurements had several advantages compared to the visual method.

1. The instantaneous resolution photograph eliminated the time involved to determine a resolution limit in the field with the visual method. A determination of P_m could be made simultaneously with the photograph.
2. The camera eliminated the effect of the "seeing" abilities of an observer on the observations.
3. Only one person instead of two was needed to obtain resolution photographs.

The results presented must be regarded as preliminary. The quality of the observations could be materially improved by the use of (1) a more powerful camera lens or (2) a more powerful microscope to analyze the photographs.

4. OBSERVATIONS OVER ICE

4.1 Introduction

Simultaneous measurements of visual resolution, scintillation and wind and temperature conditions over an ice surface on Ford Lake were begun in February 1961. Because warm weather caused rapid deterioration of the ice after two short observation periods, only limited results were reported in Part I. One of the observation periods was at night with a clear sky, low wind speed, and a smooth, snow-free ice surface. With these conditions, the vertical temperature gradient was small, P_m was low, and visual resolution was excellent. A slot size of 0.19 inch was consistently discernible over the 488 m optical path, and was among the smallest ever seen in the field experiments. Interpretation of these observations, however, was difficult because the wind was from the north, a direction unlikely to provide uniform wind and temperature conditions along the optical path because of the nearness of the adjacent land with its greatly different roughness and thermal characteristics. In the winter of 1961-1962, plans were made to resume the measurement program contingent upon the formation of a suitable ice cover on Ford Lake.

4.2 Ford Lake Observations, 1962

4.2.1 Experiment Site and Installation of Equipment -- Fig. 8 shows an aerial photograph of the section of Ford Lake important to the field experiments. The photograph was taken in the summer, but it shows the characteristics of the area which were significant for the winter measurement program. The micrometeorological equipment, photometer, and Landolt Ring chart were installed about 15 m from the north shore. The 24-power telescope used to view the resolution chart and the light source used in the scintillation measurements were installed about 458 m south of the photometer and near the south shore.

In addition to the equipment used to measure scintillation and visual resolution, the following meteorological instrumentation was installed on the ice of Ford Lake on 17 January 1962:

1. A 4-meter profile mast with thermocouples and Beckman and Whitley anemometers at 50, 100, 200 and 400 cm above ice.
2. Thermocouples at 1, 7, 14, and 28 cm depths in the ice (after 18 January).
3. A 2-meter wind profile mast with Thornthwaite anemometers at 15, 30, 75, and 150 cm.
4. Wind direction vane.

With a wind direction from the southwest quadrant, an unobstructed fetch of about 900 m existed over the ice. However, with a wind direction from any other quadrant, the adjacent land exerted serious but unknown effects on the measurement conditions.

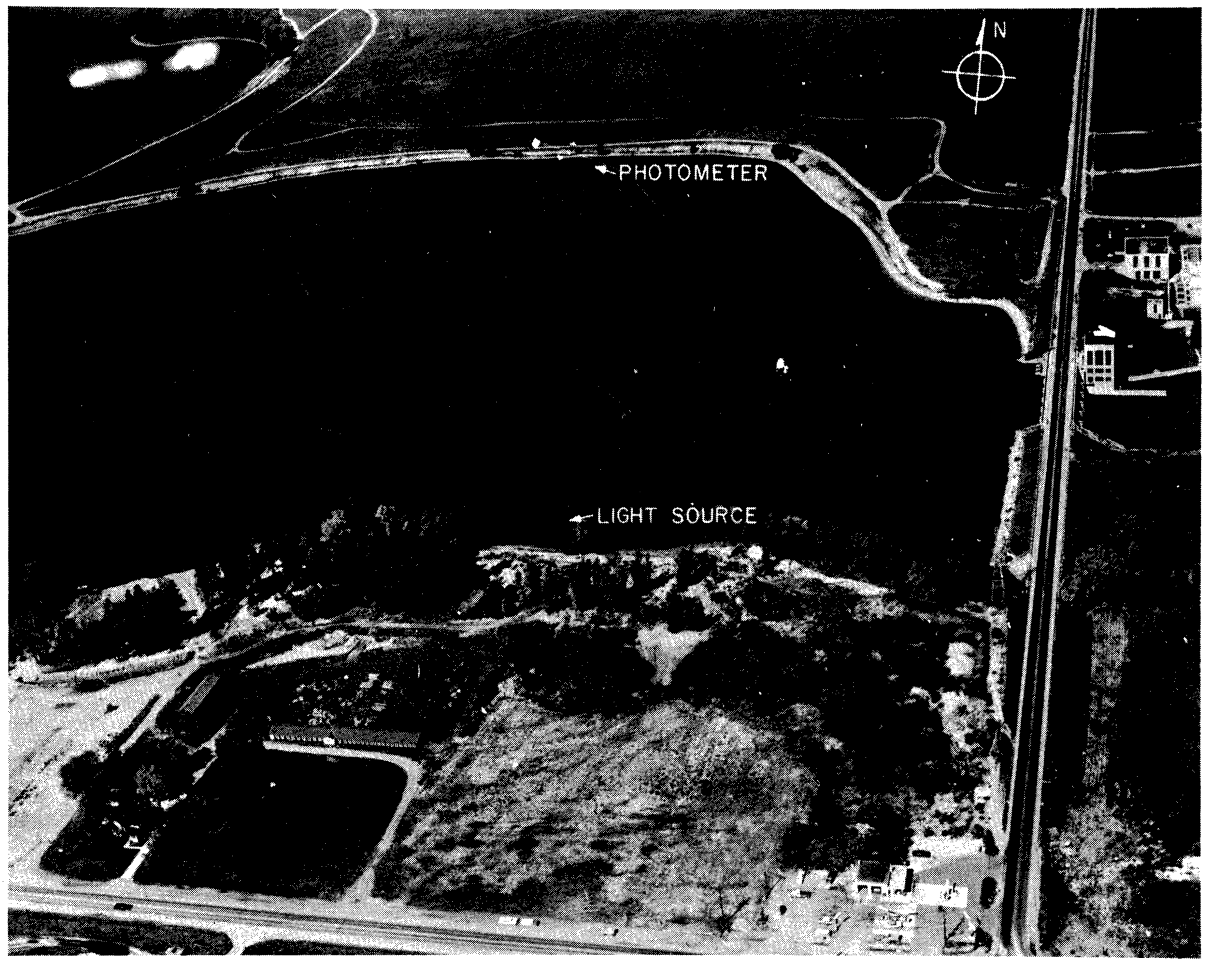

Figure 8. Aerial Photograph of Experiment Site Section of Ford Lake

4.2.2 Scintillation Equipment and Procedures -- Significant improvements in the measurement equipment were made between the time of publication of Part I, which presented the results of the 1960 and 1961 field experiments, and the 1962 and 1963 field experiments. An improved telephotometer system was designed to minimize adverse background light effects on the measurement of scintillation in daytime. The improvement consisted of replacing the photometer telescope with a set of lenses attached directly to the photometer chassis.

A second improvement was a new light source designed to produce a less divergent beam. The unit, shown in Fig. 9, consisted of a D.C. powered, pre-focused, projector lamp, two condensing lenses and a projection lens which had a diameter of about 5 cm.

The scintillation recording equipment was essentially the same as that used in previous experiments and described in detail in Part I. The fluctuations in light intensity were measured in terms of the per cent modulation of the received signal, defined as the ratio of the mean peak to peak amplitude of a fluctuating component of the signal to its average level. This quantity,

abbreviated P_m, gave a measure of the intensity of the fluctuations independently of slow changes in brightness due to attenuation by the atmosphere. The phototube signal was also recorded on magnetic tape for subsequent spectral analysis.

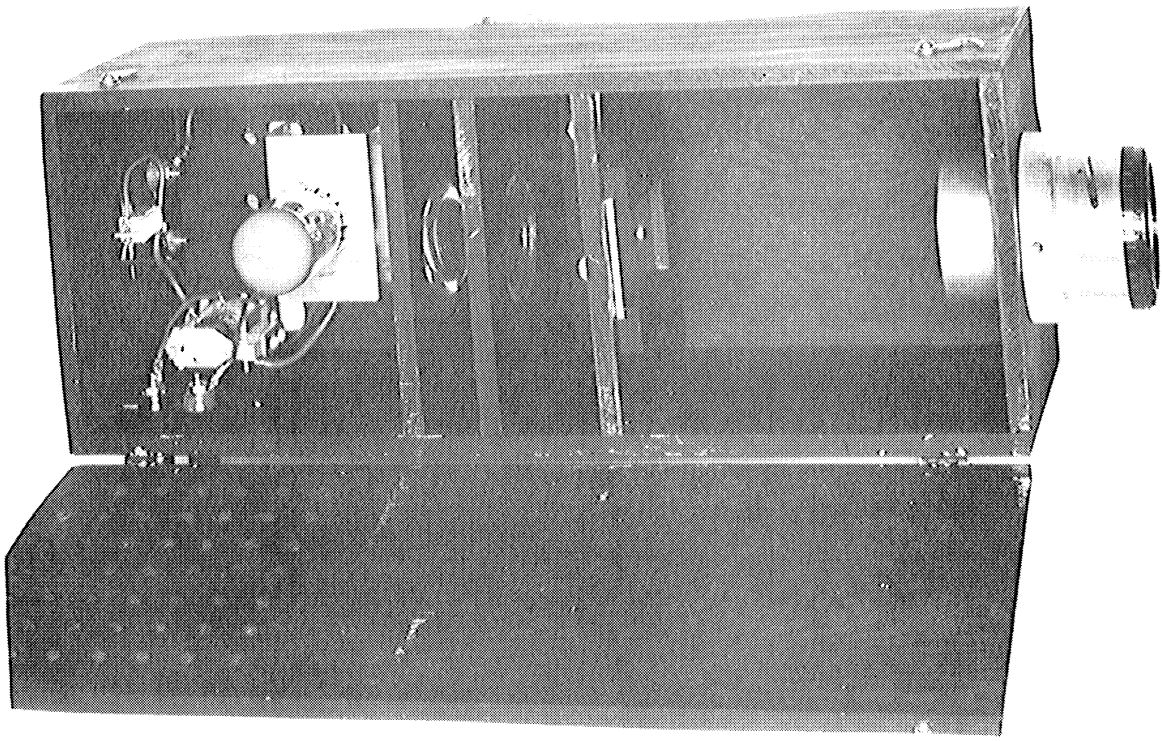

Figure 9. Improved Light Source and Photometer used in Scintillation Measurements

Because of the changes in aperture sizes of both the light source and receiver from those of the previous system, values of P_m are not directly comparable to those which comprised the various relationships discussed in Part I. The improved system indicated P_m values which were generally higher than those obtained with the previous system for similar meteorological conditions but it retained approximately the same noise level (minimum P_m value). Whereas the range of P_m values with the previous system was from about 6 to 80, that with the improved system was from about 6 to 140.

4.2.3 Observation Periods -- The first period of observations was on the night of 17 January 1962. Table II lists subsequent observation periods and brief weather summaries for each.

Table II

OBSERVATION PERIODS AND WEATHER SUMMARIES:
Ford Lake, 1962

Over Clear Ice

Date	Time(EST)	Cloudiness	Ave. Wind Vel. (mph)	Ave. Temp. °C	Ave. Dew Pt. °C	Ave. Sta. Press. (in)
Jan.						
17	2201-2400	Clear	W4	-14	-19	29.69
18	2107-2215	Clear	NW 1	-11	-16	29.61
19	1300 1500	1500 ft ovcst/ lt snow	NNE 9	-10	-12	29.37

Over Snow Covered Ice

Jan.						
23	1415-1830	3000 ft sctd	WSW 12	-5	11	29.40
	2024-2053	Hi sctd	SW 7	-7	11	29.35
24	1000-1130	Clear	SW 10	3	-7	28.97
	1600 2100	Clear	SSW 12	-1	-6	28.82
Feb.						
20	1824-2300	Hi thin Ovcst	SW 5	-5	-8	28.36

4.2.4 Results and Discussion: Wind and Temperature Profiles and Resolution Conditions over Ice -- On the night of 17 January the ice was about 32 cm thick, nearly transparent, and its surface was very smooth. The sky was clear and westerly winds of about 4 mph provided an over-ice fetch of approximately 300 m. The adjacent land surface was covered by about 2 cm of snow and the average air temperature at 1 meter was quite steady at about 14C.

Over the adjacent snow-covered ground a large inversion, high scintillation, and poor resolution would have been expected for such nighttime wind and sky conditions. However, quite the opposite was experienced over ice. Instead, a slight lapse in temperature was measured between 52 and 402 cm above the ice, scintillation was low, and resolution was good. A comparatively small slot size of 0.30 inch was discernible over the 458 m optical path throughout the two-hour observation and little change in either scintillation or meteorological conditions was observed.

Because vertical motions over a smooth ice surface are less than those over a rough land surface for equivalent conditions of thermal stratification and wind, somewhat lower scintillation intensity would have been expected over the ice than over land. What was not expected was the absence of a pronounced inversion. To explore the condition further, thermocouples were installed at 1, 7, 14 and 28 cm below the ice surface on 18 January.

It is evident that as the depth of the snow cover on the ice changed once it accumulated later in field experiments, the depth of the thermocouples in the ice changed with respect to the air-snow interface. However, because the temperature structure through the overlying snow was not known except by inference in rare cases of neutral atmospheric stability, it will be assumed later for purposes of heat flux computations within the ice that the thermocouple depths with respect to the original surface of the ice remained constant. With this assumption, the conduction of heat between specific depths within the ice will be discussed quantitatively in a later section but the effect of the snow cover on heat conduction will be described qualitatively.

Observations were resumed on the night of 18 January when the sky was clear and the ice condition similar to that on the previous night. However, the average wind velocity was only about 1 mph from the northwest. As noted above, a north wind gave an effective upwind fetch of only about 16 m between the profile mast and shore, so that the measurements were not likely to represent conditions over ice. Scintillation intensity was as steady but slightly lower than that of the previous night and resolution was better. A slot size of 0.24 inch was discernible throughout the observation period. The slightly lower scintillation and better resolution compared to the observations on 17 January were apparently due to the nearly calm wind.

The average wind profiles and air and ice temperature profiles from 2000 to 2200 EST on 18 January are shown in Fig. 10. In Figures 10 through 23 air temperature and wind speed are graphed against height above ice on a log scale; ice temperature is graphed against depth in ice on a linear scale. The surface of the ice on the linear scale coincides with the 10 cm height above the ice on the log scale. The average air temperature on 18 January is about -12C and the profile consists of an inversion of about 1.4C between 52 and 402 cm. However, between 52 cm above ice and 1 cm below the ice surface, an abrupt increase in temperature is evident. The average temperature at 1 cm below the ice surface is almost 9C warmer than that at 52 cm above ice. Also, it is 3C warmer than the maximum air temperature in the past 48 hours. Just where the air and ice temperature profiles meet at the air-ice interface is not known with any certainty. The temperature continues to increase repidly with depth between 1 cm and 6 cm in the ice. Because of the large temperature difference between these two depths, it was unlikely that the profile would be linear. The profile shown in Fig. 10 is an estimate based on experience with similar profiles in snow and soil. Below 6 cm the warming continues but at a much slower and nearly linear rate to at

least a depth of 28 cm. The wind profile shows curvature similar to the temperature profile, but neither can be accurately interpreted because of the unfavorable wind direction.

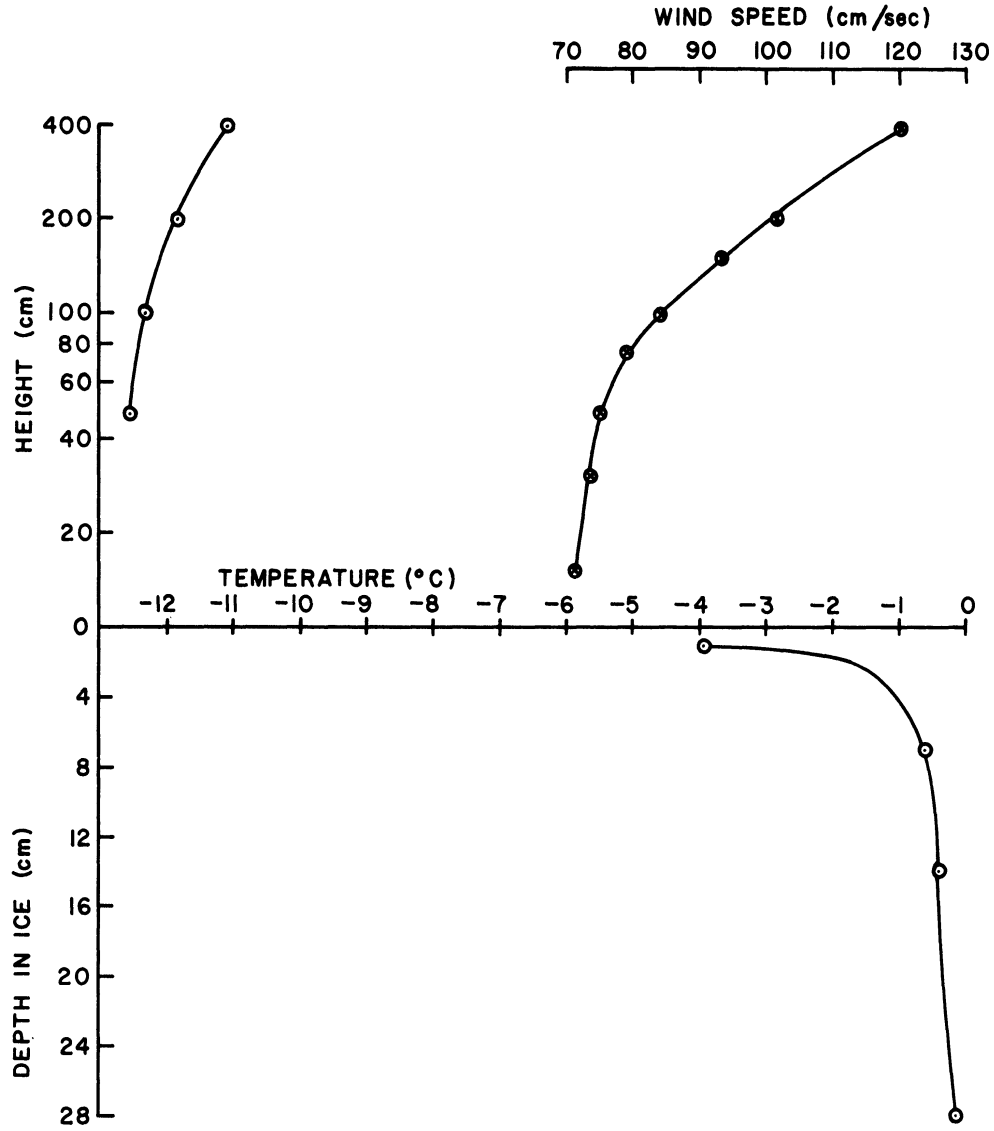

Figure 10. Wind Speed (⊗) and Air Temperature (⊙) vs. Height (Log Scale) and Temperature vs. Depth in Ice (Linear Scale), Ford Lake, 2000-2200 EST, 18 Jan., 1962

Following the observation period on 18 January, cloudiness began to increase until a dense overcast based at 1500 feet existed by 1300 EST on 19 January. Daytime observations were resumed at that time except for scintillation measurements. The wind was NNE at 9 mph, again a poor direction for meaningful interpretation of wind and temperature profiles. Fig. 11 shows a 40-minute daytime average of air and ice temperature profiles as a snowfall was beginning on 19 January. A temperature inversion of 0.3C is evident

between 52 and 402 cm above ice. Within the ice the temperature increases 5.3C between 1 and 28 cm. The temperature at 1 cm below the ice surface is 4.5C warmer than the air at 52 cm. A rather striking feature of the ice temperature profile is its linearity for this daytime overcast sky condition in contrast to the curved profile between 1 and 7 cm for a clear sky condition at night on 18 January.

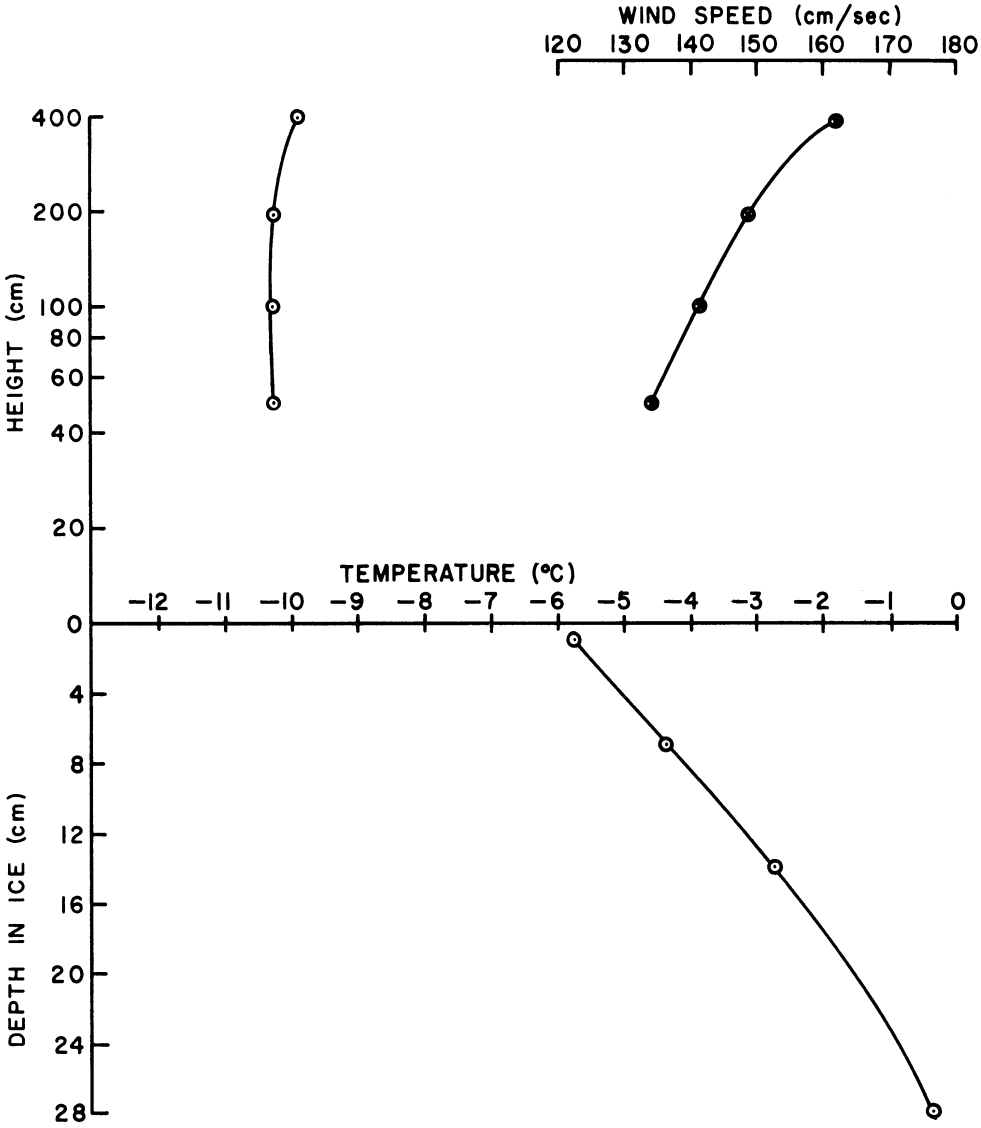

Figure 11. Wind Speed (⊗) and Air Temperature (⊙) vs. Height (Log Scale) and Temperature vs. Depth in Ice (Linear Scale), Ford Lake, 1402-1441 EST, 19 Jan., 1962

A snowfall of about 4 cm occurred overnight on 19-20 January. The ice surface remained generally snow-covered for the remainder of the winter. Additional profile measurements were obtained on 23 and 24 January when the ice surface was covered by about 2 cm of crusted snow. During both periods,

skies were generally clear and the wind direction was southwest, providing an over-snow fetch of about 700 m. Average profiles of air temperature, wind speed and ice temperatures between 2024 and 2052 EST which are typical of nighttime conditions on 23 January are shown in Fig. 12. The air temperature profile shows an inversion of about 0.1C between 50 and 400 cm. The average air temperature was -7C. The temperature at 1 cm within the ice is 3.5C warmer than that at 50 cm above the snow-covered ice. A nearly linear 3.4C increase in temperature exists between 1 and 28 cm within the ice.

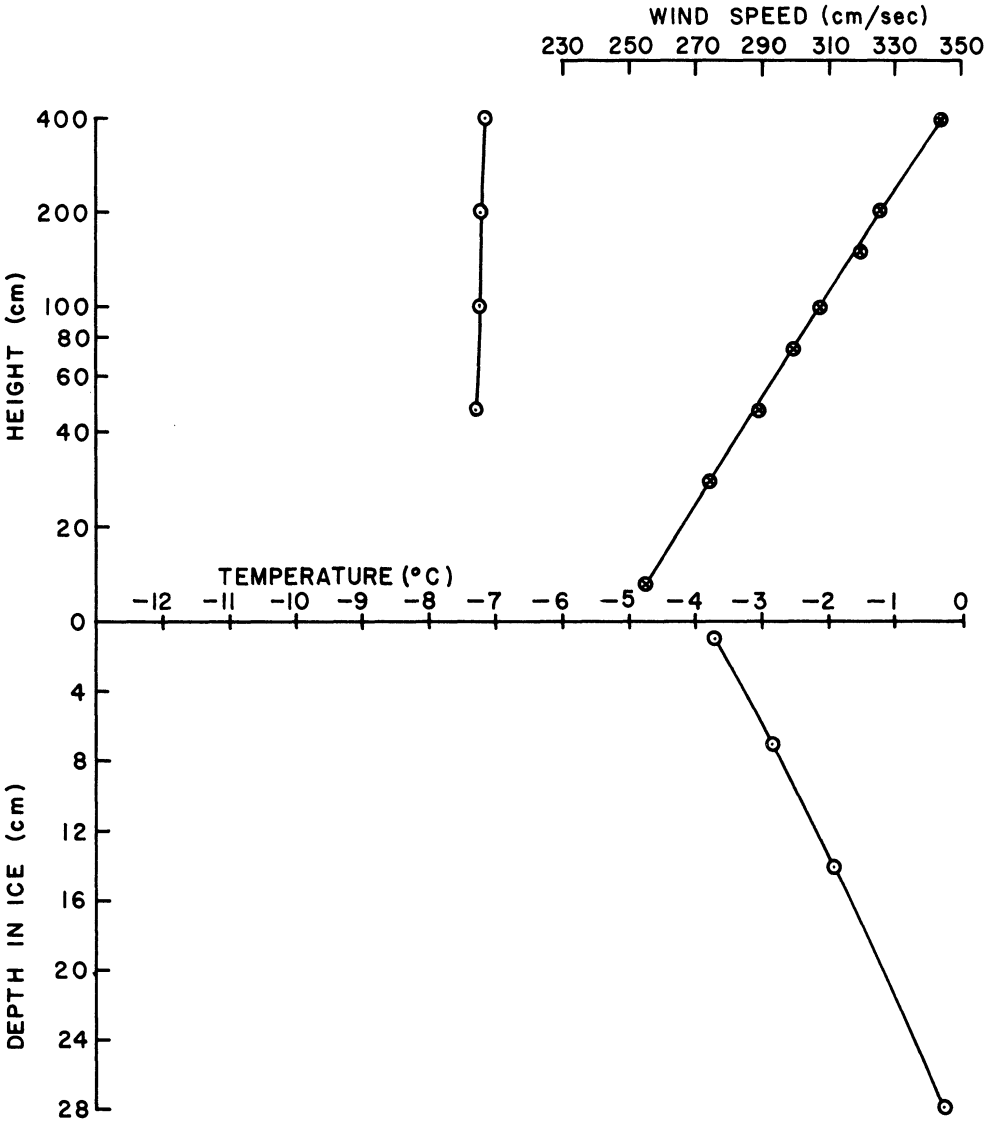

Figure 12. Wind Speed (⊗) and Air Temperature (⊙) vs. Height (Log Scale) and Temperature vs. Depth in Ice (Linear Scale), Ford Lake, 2024-2052 EST, 23 Jan., 1962

Warmer air was advected during the night of 23-24 January. The half-hour average of air and ice temperature profiles observed between 1010 and 1040 EST on 24 January is shown in Fig. 13. Average air temperature is -3.6C and

a 0.15C inversion is evident between 50 and 400 cm above 2 cm of snow on the ice. The first 10 cm of ice are colder than air temperatures in the first few meters above it even though the ice temperature at 28 cm is 2.8C warmer than at 1 cm. Warming of both air and ice occurred throughout the day with a clear sky and southwest winds. The average profiles observed between 2100 and 2144 EST are shown in Fig. 14. Average air temperature is -1.6C and a 0.5C inversion exists between 50 and 400 cm. A nearly linear temperature decrease of 2.2C occurs through the ice between 1 and 28 cm.

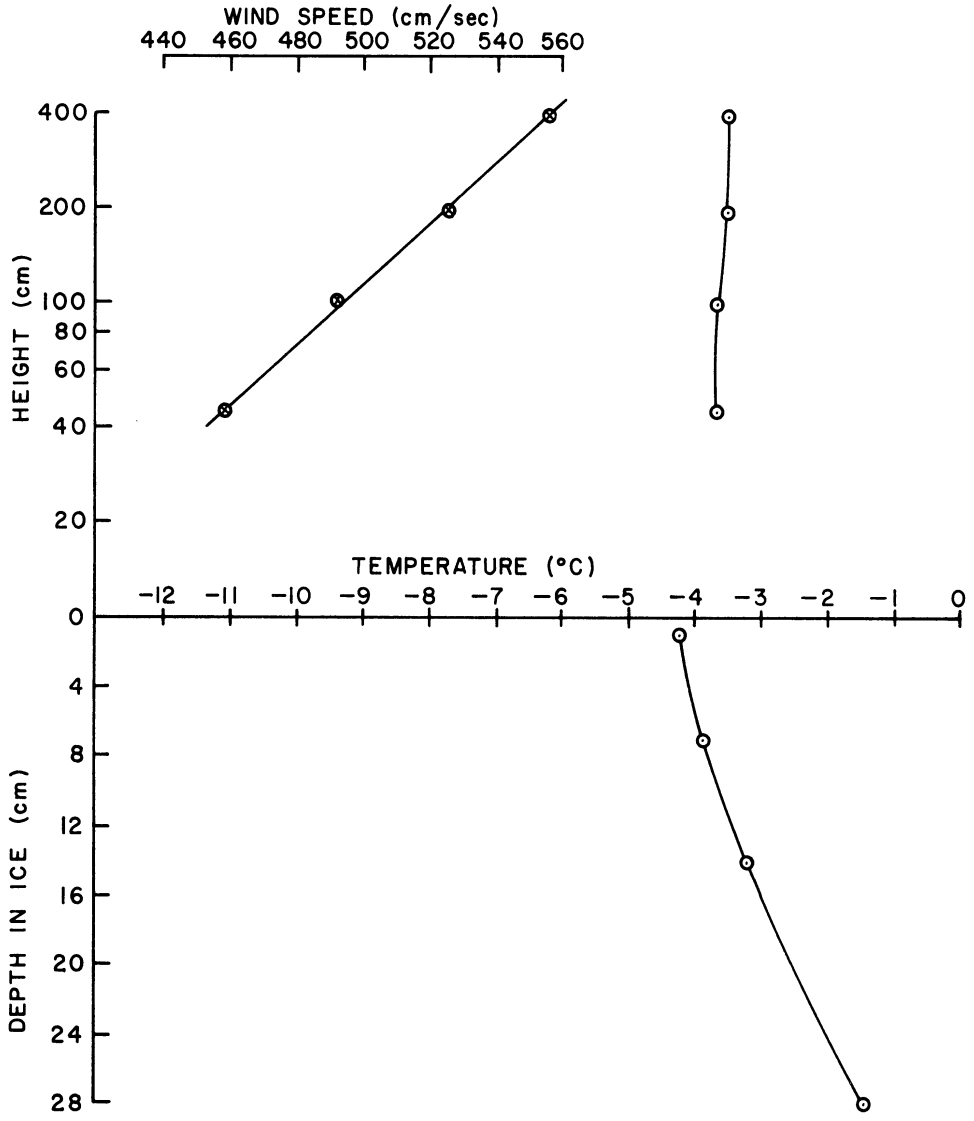

Figure 13. Wind Speed (⊗) and Air Temperature (⊙) vs. Height (Log Scale) and Temperature vs. Depth in Ice (Linear Scale), Ford Lake, 1010-1040 EST, 24 Jan., 1962

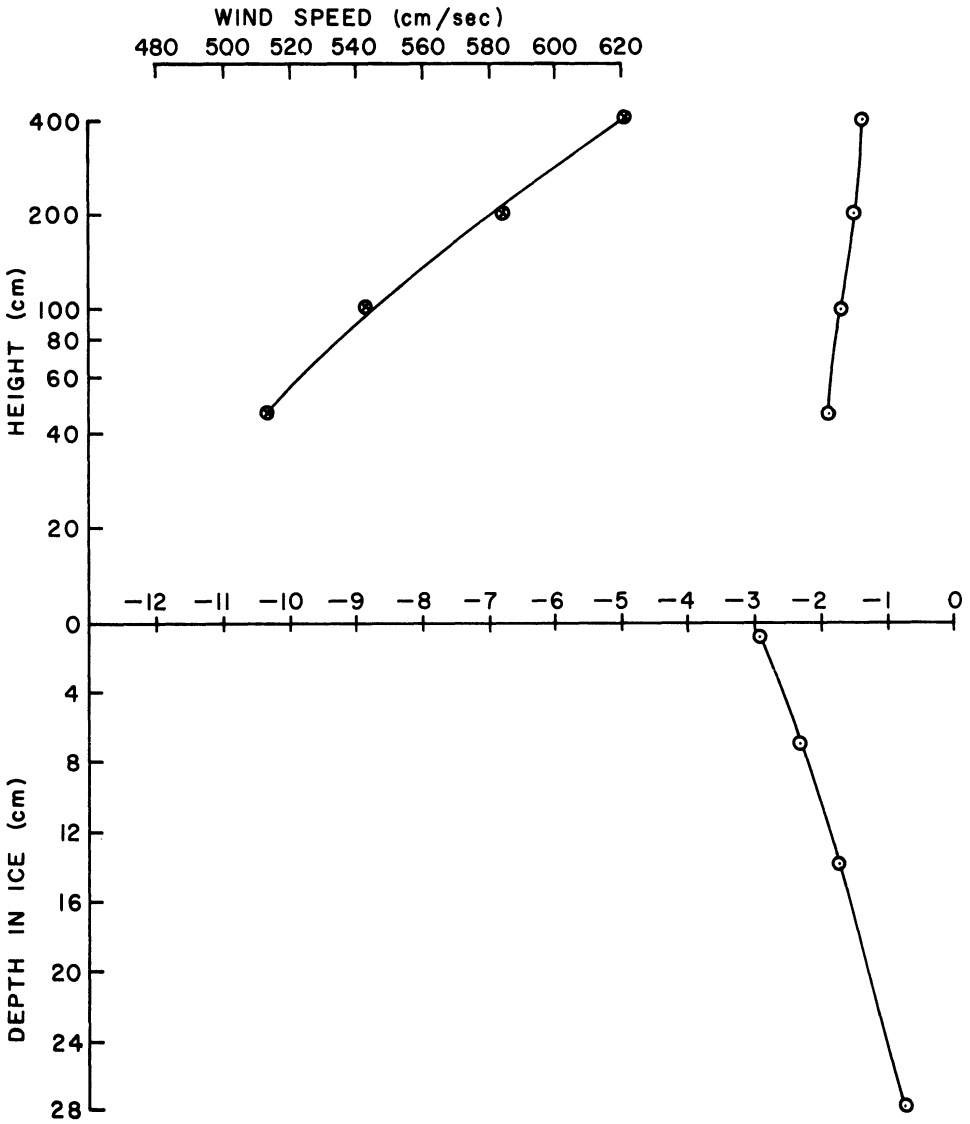

Figure 14. Wind Speed (⊗) and Air Temperature (⊙) vs. Height (Log Scale) and Temperature vs. Depth in Ice (Linear Scale), Ford Lake, 2100-2144 EST, 24 Jan., 1962

For the observation period on 23 January and that on 24 January (1010-1040 EST) nearly logarithmic wind profiles reflect the small vertical temperature differences. Although neither scintillation nor resolution measurements were made on either day, the small vertical temperature differences indicate that P_m would have been very low and resolution excellent for both observation periods.

The next period of observations was on 20 February. The ice surface was covered by about 8 to 12 cm od dense snow under a crust of consolidated sleet. The sky was initially clear, the average air temperature was about -4C and the wind velocity at 2-meters was southwest at about 2 mph. The air and ice temperature profiles are shown in Fig. 15. A 0.35C inversion exists

between 43 and 394 cm above the snow. The ice temperature is nearly isothermal at -0.5C. Scintillation was low and quite steady and resolution was good. A slot size of 0.24 inch was discernible throughout the 3 hours of measurement.

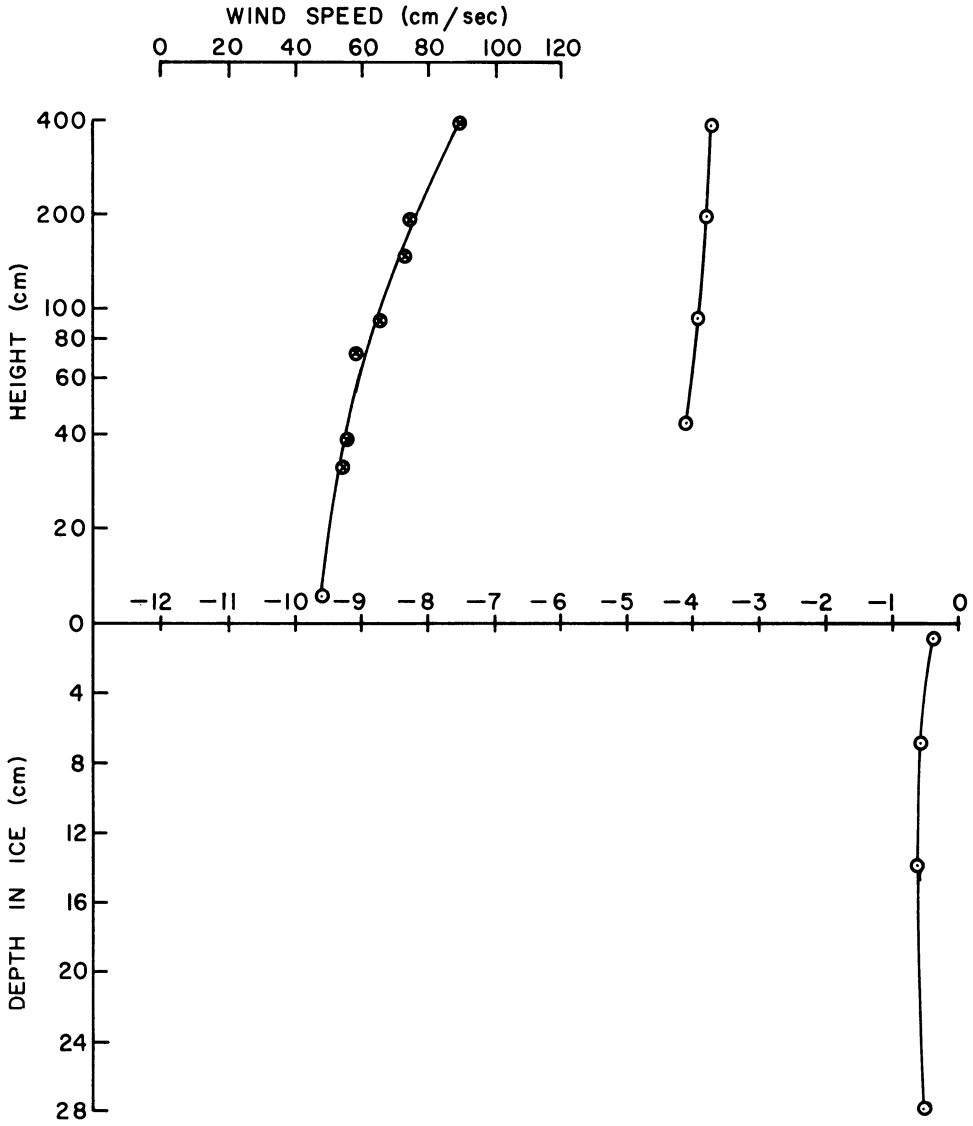

Figure 15. Wind Speed (⊗) and Air Temperature (⊙) vs. Height (Log Scale) and Temperature vs. Depth in Ice (Linear Scale), Ford Lake, 1830-1916 EST, 20 Feb., 1962

4.3 Whitmore Lake Observations, 1963

4.3.1 Experiment Site -- In the winter of 1962-63 additional observations were obtained on the ice surface of Whitmore Lake, located approximately ten miles north of Ann Arbor, Michigan, and comprising an area of about 680 acres. One of the chief advantages of this site over the Ford Lake site is the longer upwind fetch over ice for a greater range of wind directions. This feature is of major importance to meaningful interpretation of wind and

temperature profiles and scintillation data.

4.3.2 Equipment and Procedures -- Scintillation and micrometeorological equipment was installed on the ice surface of Whitmore Lake early in January. The profile instrumentation consisted of Thornthwaite anemometers for wind speed measurement and shielded thermocouple junctions for air temperature measurements at heights of 50, 100, 200, and 400 cm above the ice surface. In addition, thermocouple junctions were installed at depths of 1, 3, 6, 10, 15, 20, 30, and 40 cm below the ice surface in an area near the profile mast where the water depth was about one meter. By the time of the first observation period on 15 January the ice was 41 cm thick and it was established at that time that all thermocouples were solidly embedded in ice.

4.3.3 Observation Periods -- The periods of observations at Whitmore Lake in 1963 are listed in Table III together with representative averages of cloudiness, wind velocity, air temperature, and dew point temperature. Throughout the measurement program, the ice surface unfortunately was never completely free of snow. For the observations on 15 and 17 January, about 30% of the ice was covered by snow 3 to 4 cm deep. On 23 and 31 January, the ice was completely covered with snow about 10-15 cm deep and remained in this condition through February. Because the month of January was very cold, however, the ice consistency remained exceptionally clear as the thickness increased. For the observations in March the ice was covered by a layer of frozen slush about 8 cm deep on top of which was a layer of snow.

Table III

OBSERVATION PERIODS AND WEATHER SUMMARIES:
Whitmore Lake, 1963

Over Snow-covered Ice

Date	Time(EST)	Cloudiness	Ave. Wind Vel. (mph)	Ave. Temp. °C	Ave. Dew Pt. °C	Ave. Sta. Press. (in)
Jan.						
15	1700-2100	Clear	SW 4	-17	-21	29.44
	1100-1200	12,000 ft broken	SSW 5	-9	-15	29.47
17	1330-1520	10,000 ft thin ovcst	NNW 4	-6	-11	29.41
	1518-1624	1500 ft broken	SW 17	-19	-36	29.44
23	1812-1958	Clear	NW 10	-22	-36	29.47
	1640-1740	Hi thin sctd	SSW 8	-12	-17	29.44
31	1846-2050	Hi thin sctd	SE 4	-17	-20	29.44
Mar.						
7	1616-1706	3500 ft ovcst	SW 12	-1	-2	29.09
13	2140-2346	Clear	SW 6	-9	-11	29.41
14	1518-1616	Clear	WNW 6	+1	-2	29.47
15	1418-1444	Hi sctd	ESE 3	+2	-4	29.44

4.3.4 Results and Discussion: Wind and Temperature Profiles and Scintillation Conditions over Ice -- Average profiles of air and ice temperatures and wind speed representing the periods of observations over ice and snow-covered ice in 1963 are shown in Figures 16 through 23. The ordinate scale is the same as that in the figures discussed in Section 4.2.4.

The observation periods with the least amount of snow on the ice surface were those on 15 and 17 January when about 30% of the ice was covered by snow about 3 cm deep. The profiles for these periods are shown in Figures 16 and 17. Although observations on 15 January were made at night and those on 17 January during daytime, each air temperature profile showed a slight lapse (decrease with height) between 50 and 400 cm. In the former period, the lapse was 0.2C and the temperature at 1 cm in the ice was about 5C warmer than the average -17C air temperature at 50 cm. In the latter case, the lapse was 0.5C and the ice temperature 1 cm deep was 1C warmer than the average -9C air temperature at 50 cm. A linear increase of 12.5C existed between 1 and 40 cm on 15 January and a slightly non-linear increase of 8C existed on 17 January. On both days, scintillation intensity was extremely low and P_m ranged between 5 and 15 per cent, a condition substantiated by the small vertical temperature gradients above the ice.

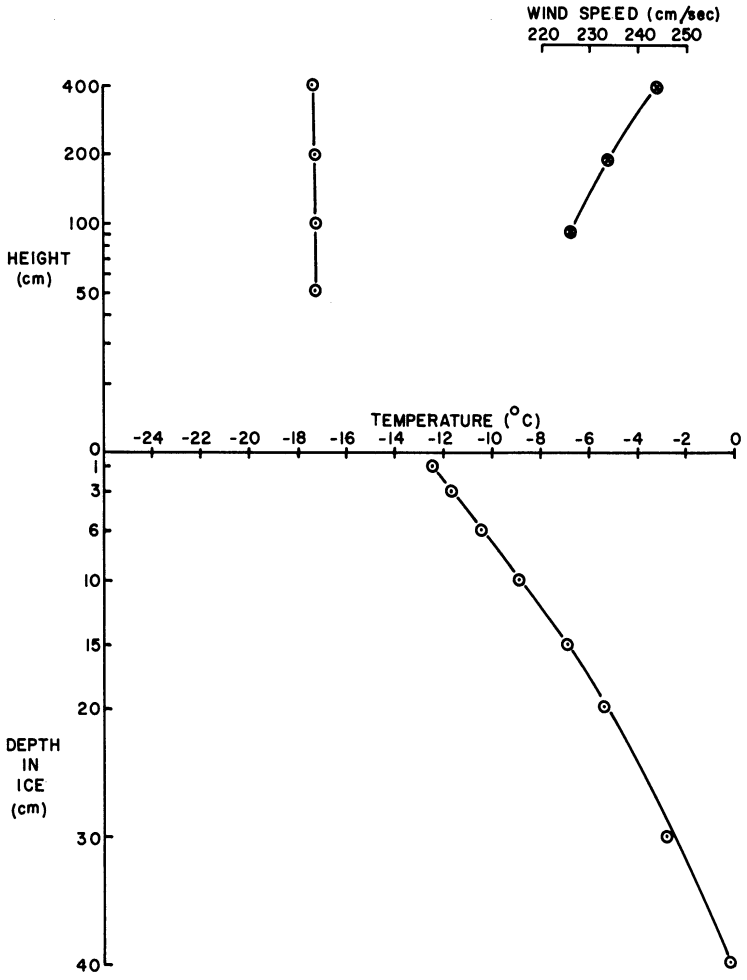

Figure 16. Wind Speed (⊗) and Air Temperature (⊙) vs. Height (Log Scale) and Temperature vs. Depth in Ice (Linear Scale), Whitmore Lake, 2030-2100 EST, 15 Jan., 1963

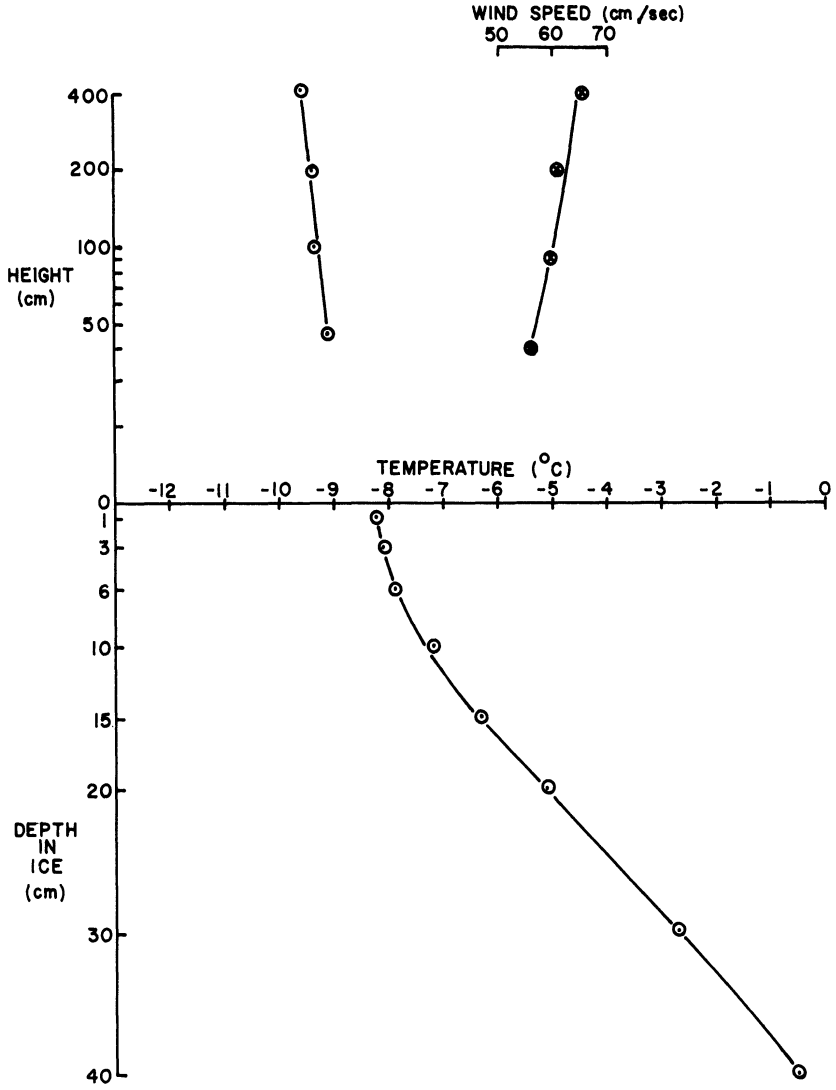

Figure 17. Wind Speed (⊙) and Air Temperature (⊙) vs. Height (Log Scale) and Temperature vs Depth in Ice (Linear Scale), Whitmore Lake, 1100-1200 EST, 17 Jan., 1963

The period of observations with the coldest air temperatures was on the night of 23 January when about 10 cm of snow covered the ice. A half hour average of the profiles for this period is shown in Fig. 18. The nearly neutral air temperature profile between 50 and 400 cm is the result of the high wind speed, which averaged about 450 cm sec^{-1} (10 mph) at one meter. The air temperature at 50 cm averaged about -22C and the temperature at 1 cm below the ice surface was -2.3C, or about 20C warmer. The ice temperature continued to increase slowly with depth at an approximately linear rate to a temperature near 0C at 40 cm. Again, scintillation intensity was extremely low and P_m averaged about 8.

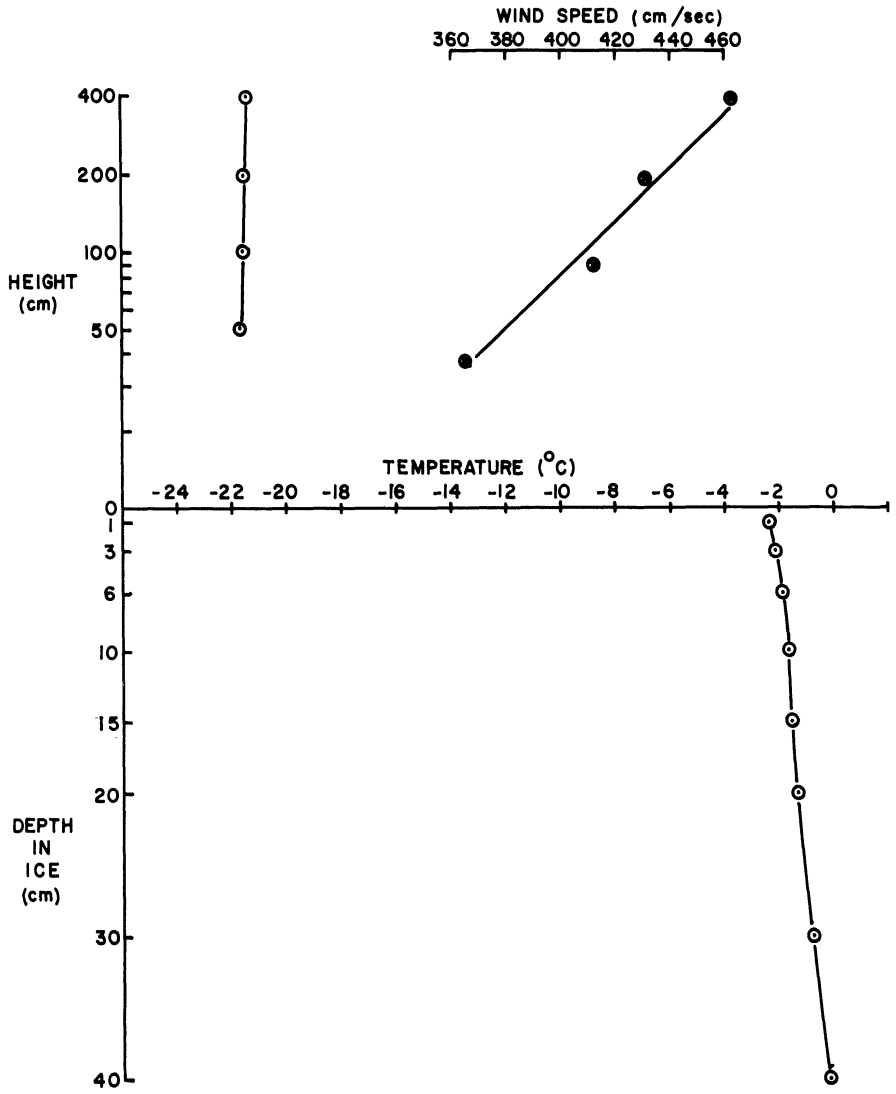

Figure 18. Wind Speed (⊗) and Air Temperature (⊙) vs. Height (Log Scale) and Temperature vs. Depth in Ice (Linear Scale), Whitmore Lake, 1820-1850 EST, 23 Jan., 1963

A similar weather condition, except for a much lower wind speed, was observed on 31 January for which a half-hour average of the profiles is shown in Fig. 19. The snow depth on the ice was 12 cm. However, an inversion which averaged about 2C existed between 50 and 400 cm and represents the largest inversion observed in the experiments. This evidently occurred because of the low wind speed ($\sim$ 1 mph), clear sky, and deeper snow on the ice. The air temperature at 50 cm was -17C and that at 1 cm in the ice was -4.5C, or about 13C warmer. The general shape of the ice temperature profile was similar to that of 23 January.

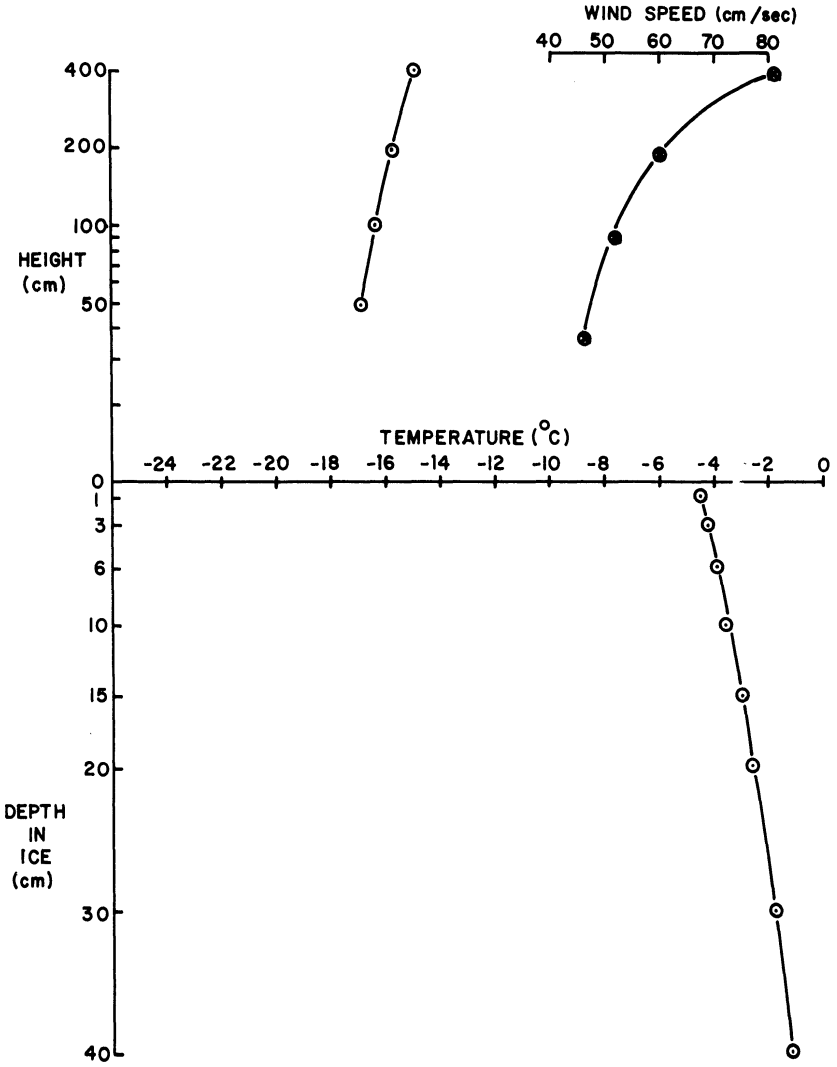

Figure 19. Wind Speed (⊗) and Air Temperature (⊙) vs. Height (Log Scale) and Temperature vs. Depth in Ice (Linear Scale), Whitmore Lake, 2000-2030 EST, 31 Jan., 1963

Scintillation intensity during the period of observations on 31 January was the most variable and occasionally the highest ever observed in the experiments over ice. Values of P_m ranged from 4 to 36. The behavior was somewhat similar to that observed with a moderately large inversion and very low wind speeds over ground or snow-covered ground, in that small increases in wind speed often caused a transition from a period with very little scintillation to short intervals of more intense scintillation. This behavior was similar to that discussed in the Part I for observations at KFS over snow about 50 cm deep, and supported the idea of the presence of internal gravity waves with frequent breaking to brief periods of turbulent flow.

A period with similar conditions except for generally warmer air and ice temperatures was observed on the night of 13 March, the profiles for which are shown in Fig. 20. About 12 cm of snow, frozen slush, and some liquid water comprised the layer on top of the solid ice. The ice temperature profile was nearly isothermal at -0.2C between 1 cm and 40 cm.

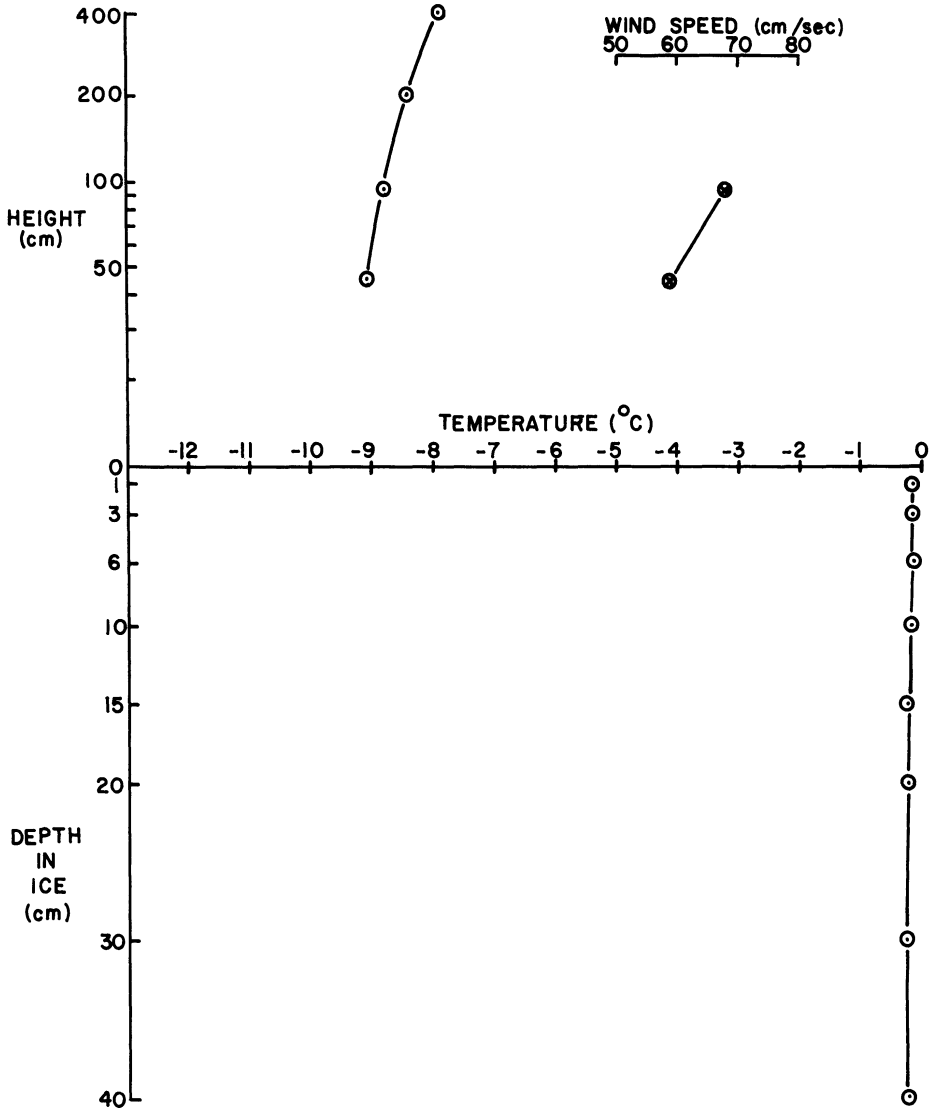

Figure 20. Wind Speed (⊗) and Air Temperature (⊙) vs. Height (Log Scale) and Temperature vs. Depth in Ice (Linear Scale), Whitmore Lake, 2300-2330 EST, 13 Mar., 1963

The three daytime periods in March are similar to each other with respect to low scintillation intensity but different with respect to their temperature profiles which are shown in Fig. 21, 22, and 23. On 7 March, with a temperature of -1.3C at 50 cm, a temperature lapse of 0.3C between 50 and 400 cm was observed. The ice temperature profile was nearly isothermal at -0.1C. On 14 and 15 March slight inversions were observed. This condition was expected

because the air temperatures of +1.1C and +1.4C at 50 cm on 14 and 15 March, respectively, indicated that warmer air was being advected. Since the foot of the temperature-height curve is anchored at 0C for a melting snow surface during air temperatures above freezing, temperature must increase with height at least in the layer near the snow. However, the inversion was not large enough to cause appreciable scintillation and Pm averaged between 5 and 15 on both days. It is conceivable that scintillation during conditions of warm air advection over melting ice could be very intense, since a strong inversion could be maintained all during the melting process.

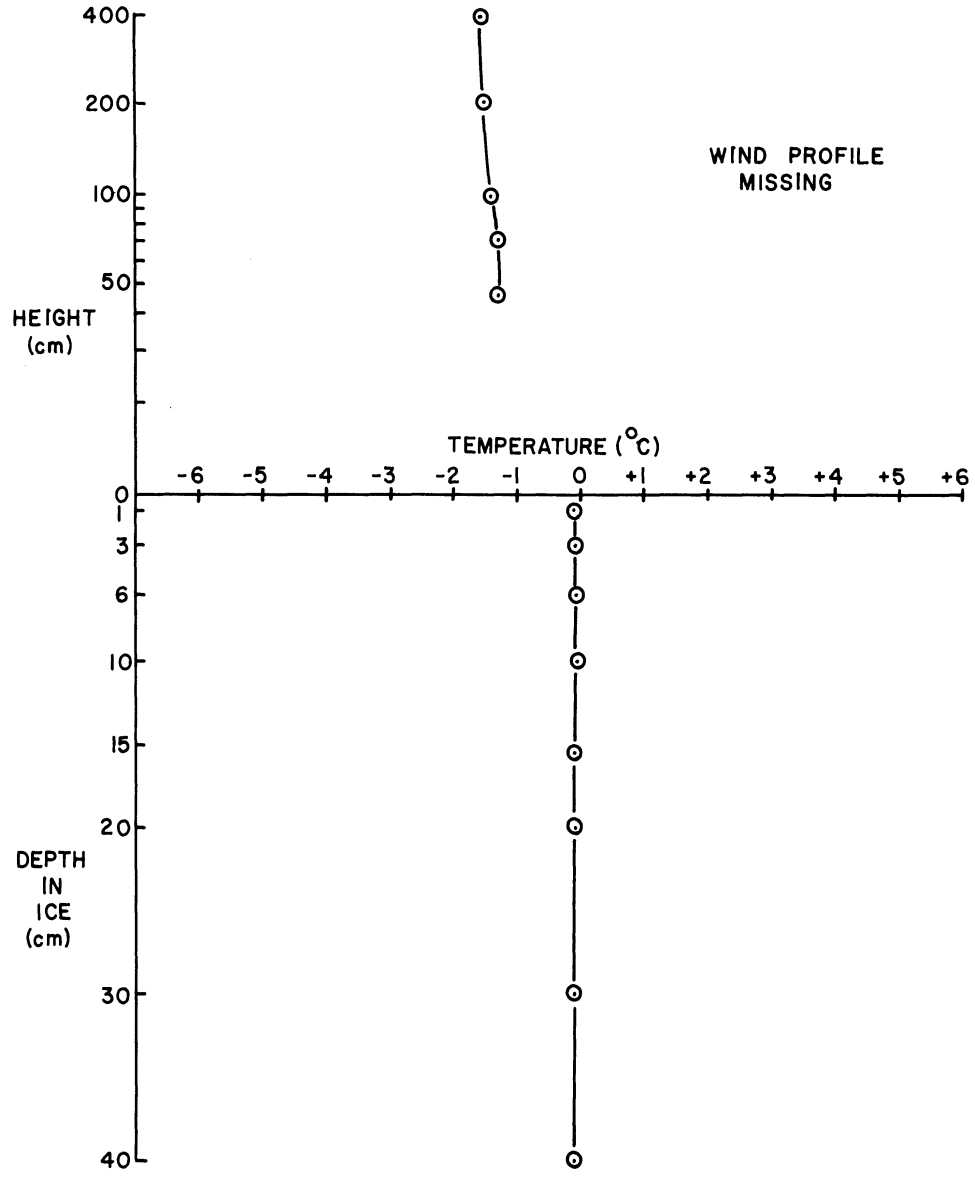

Figure 21. Wind Speed (⊗) and Air Temperature (⊙) vs. Height (Log Scale) and Temperature vs. Depth in Ice (Linear Scale), Whitmore Lake, 1654-1714 EST, 7 Mar., 1963

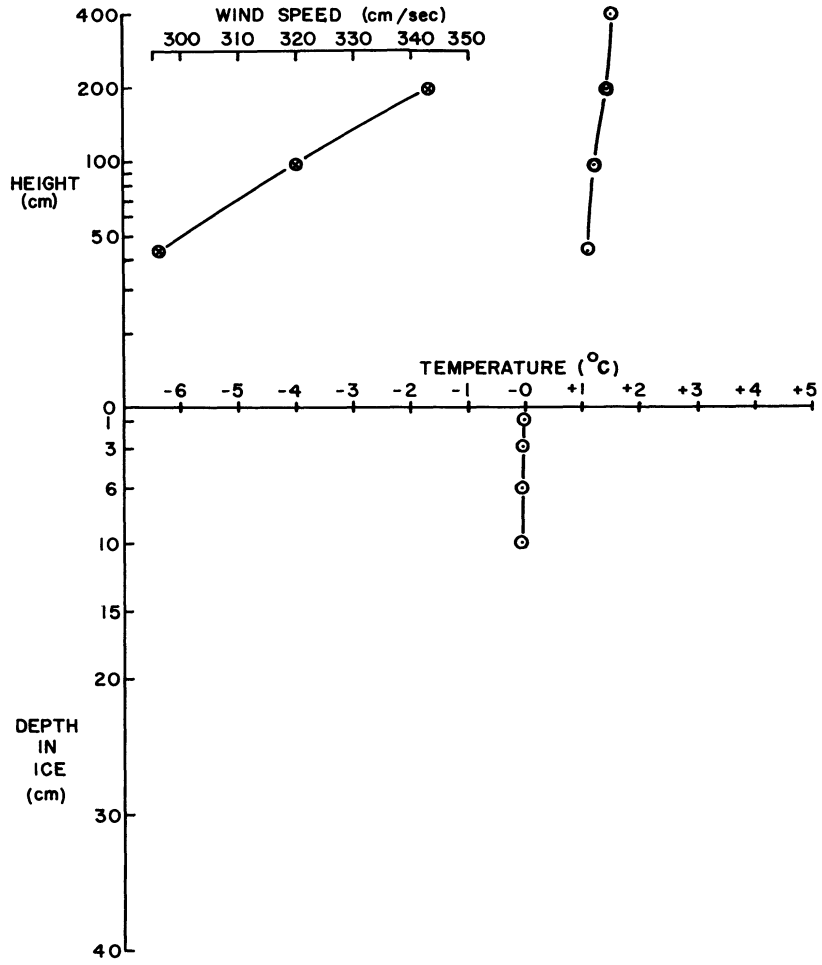

Figure 22. Wind Speed (⊗) and Air Temperature (⊙) vs. Height (Log Scale) and Temperature vs. Depth in Ice (Linear Scale), Whitmore Lake, 1530-1550 EST, 14 Mar., 1963

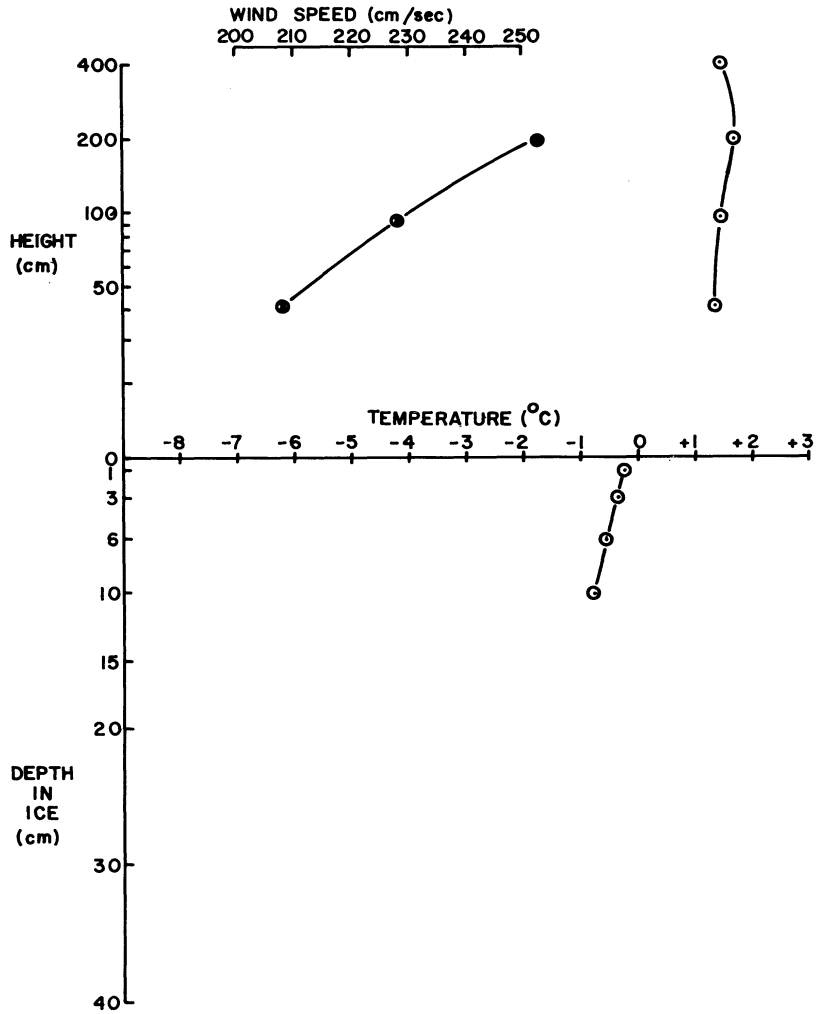

Figure 23. Wind Speed (⊗) and Air Temperature (⊙) vs. Height (Log Scale) and Temperature vs. Depth in Ice (Linear Scale), Whitmore Lake, 1426-1442 EST, 15 Mar., 1963

4.4 Conduction of Heat in Ice

It is believed that one of the main reasons for the absence of pronounced inversions over clear ice and the resulting low scintillation intensity was the relatively large amount of heat conducted to the ice surface from below. An estimation of the heat conducted through the ice at 4 cm depth may be obtained from the following equation:

$$q_{4\ cm} = -\lambda\ (\Delta T/\Delta z)_{4\ cm}$$

where q = heat flux (ly min^{-1})
λ = thermal conductivity of ice ($\cong$ 0.33 g cal cm^{-1} deg^{-1} min^{-1})
T = ice temperature (deg C)
z = depth in ice (cm)

The thermal conductivity of ice, assumed to be constant with depth, was obtained from the recent work of Ratcliffe (1962).

The periods in 1962 and 1963 for which computations of conductive heat transfer were made are listed in Table IV. Ice temperatures at 1 cm and 7 cm, temperature gradients in the ice, and heat flux data are given for each period. The temperature gradient was obtained by subtracting the ice temperature at 1 cm from that at 7 cm and dividing by 6. A negative value of heat flux means a transfer of heat upward.

Table IV

CONDUCTIVE HEAT TRANSFER DATA FOR ICE

Date	Time (EST)	$T_{7\ cm}$ (C)	$T_{1\ cm}$ (C)	$\Delta T/\Delta z$ C cm^{-1}	Conductive Heat Transfer ly min^{-1}
1962					
18 Jan.	2050-2130	-0.33	-3.90	-0.595	-0.193
19 Jan.	1402-1441	-4.34	-5.72	-0.185	-0.060
23 Jan.	1716-1822	-2.10	-3.01	-0.150	-0.049
24 Jan.	1010-1040	-3.88	-4.25	-0.060	-0.019
	1858-1958	-2.18	-2.78	-0.100	-0.032
20 Feb.	1958-2248	-0.24	-0.07	+0.050	+0.016
1963					
15 Jan.	1945-2035	-10.47	-12.43	-0.327	-0.106
17 Jan.	1336-1556	-1.94	-2.06	-0.014	-0.005
23 Jan.	1520-1600	-1.94	-2.24	-0.050	-0.017
31 Jan.	1710-1730	-4.58	-4.73	-0.050	-0.017
7 Mar.	1654-1714	-0.09	-0.14	-0.010	-0.003
13 Mar.	2258-2338	-0.17	-0.16	+0.002	+0.001
14 Mar.	1518-1616	-0.03	-0.02	+0.001	+0.0003
15 Mar.	1418-1444	-0.60	-0.23	+0.060	+0.019

The greatest upward heat flux through the 4 cm depth occurred on 18 January 1962 and was about -0.2 ly min^{-1}. It must be noted, however, that this computation was based on a linear temperature profile between 1 and 7 cm. As mentioned previously, the profile was not likely to be linear between these depths and the best estimate of what it should be was shown in Fig. 10. It is evident from the profile that at depths closer to the surface than 4 cm, the heat flux should be even greater than 0.2 ly min^{-1}.

The magnitude of heat flux in this example may be appreciated by comparing it to some extreme values of surface heat flux obtained for soil and snow. From the data given by Portman (1954) for summertime observations at O'Neill, Nebraska, the maximum upward heat flux reaching a sandy loam soil surface at night was about 0.09 ly min^{-1}. For snow, a high value is about 0.03 ly min^{-1} (Liljequist, 1957). Thus, the results of one computation of heat conduction during a nighttime condition with clear snow-free ice, a clear sky and air temperature well below freezing indicate that the heat flux reaching the ice surface exceeds high values for soil and snow.

Indications are, furthermore, that heat conduction in the ice was large enough to compensate for much of the net loss of heat at the ice surface by long wave radiation exchange, even though the heat lost in this manner is optimum during nights with clear skies. For example, the black-body radiation for -4 C, the temperature at a depth of 1 cm on January 18, 1962, would be 0.43 ly min^{-1} and if the atmospheric radiation were, say, 0.23 ly min^{-1}, a reasonable estimate (see Portman and Ryznar, 1961, Fig. 3), the net radiation heat loss would be on the order of 0.2 ly min^{-1}. At the same time, a reasonable estimate for the turbulent heat transfer from the air would be about 0.01 ly min^{-1} (Liljequist, 1957) so that for these conditions, ice heat conduction (0.19 ly min^{-1}) was sufficiently great to prevent large inversion formation.

As can be seen in Table IV the upward heat flux decreased from 0.19 ly min^{-1} on 18 January to 0.06 ly min^{-1} on 19 January 1962 as low cloudiness increased gradually to a dense overcast. The ensuing snowfall on 19 January and the snow cover on the ice for the remainder of the winter maintained smaller average temperature gradients in the ice and smaller heat fluxes until a nearly isothermal condition at 0C was measured late in February. In general, as the snow depth on the ice increased, the heat flux through the ice decreased.

For the observations in 1963, the maximum heat transfer was once again observed with the least amount of snow on the ice. On 15 January, with patches of snow about 3 cm deep on the ice, 0.11 ly min^{-1} was conducted upward through the 4 cm ice depth. On 17 January with the same amount of snow on the ice, the heat flux was only 0.005 ly min^{-1}. However, the latter value is based on daytime measurements obtained at higher air temperatures with a clear sky.

The period of observations which illustrates the insulating ability fo the snow on the ice most spectacularly was that obtained on the night of 23 January when about 10 cm of snow covered the ice. As discussed earlier, the ice temperature in the upper layers was about 20C warmer than that of the air during this period. In spite of the large ice-snow-air temperature difference, the ice temperature profile was nearly linear and the heat flux was only about 0.02 ly min^{-1} upward.

The largest temperature gradient evidently was in the upper few centimeters of the snow on the ice and could be inferred from profiles of the air and ice temperatures graphed on linear scales. Such a procedure was believed to be quite accurate in this case because the high wind speed maintained a high degree of homogeneity in air properties within the first few meters of the snow surface. An indication of this is the nearly neutral air temperature profile. Because of this condition, the air temperature profile was extrapolated to the snow surface and resulted in a temperature of -21.5C. From the -21.5C snow surface temperature to the -2.6C temperature at the ice-snow interface, the average temperature gradient within the 8 cm of snow was about 2.5C cm^{-1}. Assuming a thermal conductivity of snow of 0.0252g cal C^{-1} cm^{-1} min^{-1} (Snow Hydrology, 1956) the heat flux upward through the snow was about 0.06 ly min^{-1}.

The heat flux through the 4 cm ice depth for the remaining periods in Table IV was generally 0.02 ly min^{-1} or less. The snow cover remained at least 12 cm deep and gradually metamorphosed into a frozen slush condition early in March. On 15 March the direction of heat transfer was reversed and heat was conducted downward through the 4 cm depth. This was apparently due to seepage of warm rain water which fell during the night prior to the observations.

The above discussion indicates that either (1) a significant amount of snow (at least 10-12 cm) must accumulate on the ice or (2) the ice must be sufficiently thick before the thermal characteristics of the system are similar to those of ground and snow-covered ground in regard to the overall effects on the formation of inversions and the resulting conditions of scintillation and resolution.

4.5 Summary

The significance of the investigation over ice becomes evident by summarizing the observations and comparing them to the results obtained over a snow field about 0.5 m deep at KFS discussed in Part I. The following statements apply to meteorological and resolution conditions over ice which is between 30 and 50 cm thick.

(1) With temperatures well below freezing, a suitable wind fetch, smooth clear ice, and a clear sky, the temperature difference between 50

and 400 cm above ice did not exceed 1C regardless of wind speed or time of day. As a result, visual resolution over the 458 and 488 foot optical path in 1961 and 1962, respectively, was such that slot sizes of 0.24 inches or smaller were always discernible.

(2) Over ice covered with 3-8 cm of snow and with wind, sky and temperature conditions similar to those in (1), average temperature differences between 50 and 400 cm above the snow were slightly greater than those over snow-free ice. In mid-winter, an inversion was more common than a lapse in temperature both at night and during daytime. Resolution conditions were similar to those observed over snow-free ice.

Resolution conditions observed over both smooth ice and snow-covered ice were much better and steadier than those observed over snow-covered ground at KFS. At KFS, the smallest visible slot size was 0.24 inch or larger over a 543 meter optical path as opposed to 0.24 inch or smaller observed over ice. Also, the variability in resolution during clear nights with very light winds was generally less over ice or snow-covered ice than over snow-covered ground.

5. WILLOW RUN FIELD STATION OBSERVATIONS, 1962

5.1 Introduction

Cancellation of the 1962 measurement program over ice was forced by the onset of warm weather in February. The equipment was removed from the ice and installed at the field station at Willow Run Airport. The only equipment change in the transferral was in the profile instrumentation. Instead of the 4-meter mast with wind and temperature sensors at heights of 50, 100, 200 and 400 cm, a 10 meter mast was designed and installed at the field station with sensors at approximately 25, 50, 100, 200, 400, 600, 800 and 1000 cm above the surface. After a wind tunnel calibration, the more sensitive Thornthwaite anemometers were placed at the lower four heights and Beckman and Whitley anemometers at the upper four. Identical temperature sensors were used at all heights. The optical path was 543 m long and 1 meter high. The first period of observation was on 1 March over snow-covered ground and was discussed in Section 2.4. Observations and weather summaries for additional periods are given in Table V. From the observation period on 27 March to that on 17 April the ground was snow-free and covered with dormant grass about 3 cm high. On 14 and 16 May, grass 14-18 cm high covered the field.

Table V

OBSERVATION PERIODS AND WEATHER SUMMARIES:
Willow Run Field Station, 1962

Date	Time(EST)	Cloudiness	Ave. Wind Vel. (mph)	Ave. Temp. °C	Ave. Dew Pt. °C	Ave. Sta. Press. (in)
Mar.						
1	2100-2200	Clear	NNE 6	-13	-22	29.84
27	1752-2138	Clear	WNW 6	+10	-3	29.23
Apr.						
3	1500-1620	Hi thin Sctd	W 12	+9	-7	29.63
	1742-2112	Hi thin Sctd	SW 7	+4	-7	29.65
10	1400-1600	Clear	W 18	+14	-8	29.24
17	1346-1510	4000 ft Sctd plus Hi ovcst	W 12	+11	-8	29.30
May						
14	1045-1155	Hi thin Sctd	WSW 20	+32	+14	29.25
16	2030-2215	Clear	SSW 5	+24	+17	29.38

In the following analysis, scintillation per cent modulation (P_m) is related to meteorological conditions. As mentioned in Section 4.2.2, values of P_m in the 1962 field experiments are not directly comparable to those discussed in Part I. The improved system indicated P_m values which were generally higher than those obtained with the previous system for similar scintillation conditions but it retained approximately the same noise level (minimum P_m value).

5.2 Results and Discussion

5.2.1 Scintillation and Average Wind Speed -- In Part I the influence of wind speed (at 2-meters) on scintillation over snow for conditions of stable stratification was discussed. The results showed that P_m (1) increased sharply with an increase in wind speed from calm up to about 2-3 mph (2) remained nearly steady up to a speed of about 5 mph and (3) gradually decreased at wind speeds above 5 mph.

The results obtained over the grass surface are shown in Fig. 24 for both nighttime inversion and daytime lapse cases. The data were grouped according to wind speed intervals of 0.9 mph and each point is plotted at the mid-point of the wind speed interval. The number of two-minute periods averaged for each point is indicated.

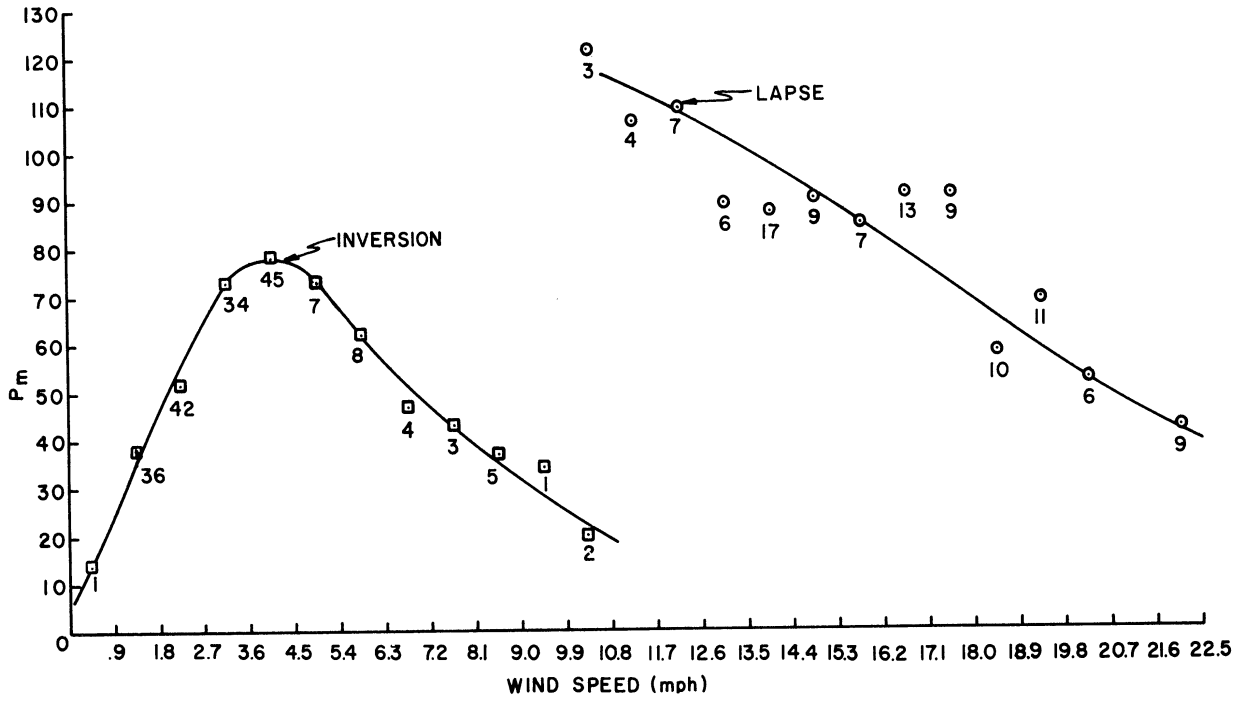

Figure 24. Per Cent Modulation vs. Wind Speed at 2 Meters for Lapse (⊙) and Inversion (⊡) Conditions over Grass

The variation of P_m with wind speed for the nighttime inversion condition corresponds closely to the variation of visual resolution with wind speed for similar conditions over snow (See Fig. 2, Section 2.2.2). P_m increased nearly linearly from a minimum of about 6 with a calm wind to about 73 at a speed of about 3 mph and to a maximum of 78 at a speed of about 4 mph before gradually decreasing. The values of P_m at speeds of 3 mph and at 5 mph were nearly equal. Above about 5 mph the gradual decrease in P_m continued, and at speeds greater than about 12 mph it again approached a minimum of about 5, which was considered to be the noise level of the system. In Fig. 2, it can be seen that visual resolution deteriorated up to a speed of about 4 mph and gradually improved at high wind speeds.

For daytime lapse conditions, data were obtained between wind speeds of about 10 and 20 mph. Values of P_m decreased from about 121 to 37 between the two speeds, respectively.

From these values, it isevident that with a clear sky, scintillation was more intense at the higher wind speeds in daytime than it was at night. For example, at a speed of 10 mph, P_m was about 20 at night and about 120 in daytime. At a speed as high as 22 mph in daytime, P_m had not decreased to a minimum value whereas at a speed of about 12 mph at night the approximate noise level of the system had been reached.

Many factors are responsible for the difference between the two curves, but in general the difference in net radiation between day and night is probably the most important. Near midday, when heating of the ground by the sun is at a maximum, the largest decrease in air temperature with height (temperature lapse) normally occurs. The ability of the sun not only to replenish but also to exceed the net heat loss from the ground surface even at high wind speeds keeps the ground surface warmer than the air and thus sustains a temperature lapse.

At night, the ground surface cools by net radiation loss and temperature increases with height (temperature inversion). In order for the ground surface to maintain the inversion above it at higher wind speeds, it must cool at a rate which will keep it colder than the air. However, at higher wind speeds the net heat loss of the surface at night is not sufficient to maintain as large a vertical temperature gradient as the heat gain can in daytime.

The fact that above about 4 mph P_m is observed to decrease with increase in wind speed, in both inversion and lapse conditions, does not conflict with the basic idea stated previously that scintillation should increase with increase in wind speed, other things remaining constant. The observed decrease in P_m reflects the fact that vertical temperature gradients are inversely related to wind speed, other things being constant. As noted above, vertical temperature gradient information is not routinely available so that the wind speed relationships shown in Figure 12 and in Figure 9 of Part I provide

useful guides for estimating visual resolution and scintillation conditions from standard weather data.

5.2.2 Scintillation and Richardson Number -- In Part I a relationship between P_m per unit vertical temperature difference between 1 and 2 m and Richardson number (Ri) for the observations made in inversion conditions over snow was discussed. If it is assumed that Ri characterizes the intensity of turbulence it should also characterize the intensity of scintillation for a given mean temperature gradient. In the discussion of the relationship it was pointed out that the change in the slope of the curve at Ri = 0.35 was taken as evidence in support of the idea of a change from turbulent flow at values less than 0.35 to laminar flow with occasional intervals of turbulence at values greater than 0.35.

The results obtained over ground are shown in relation to Ri in Fig. 25 for both temperature lapse (unstable) and inversion (stable) cases. The number of two-minute periods averaged for each point is indicated. For reference, the dashed line in the inversion case is the relationship observed over snow. As would be expected, because of the more sensitive scintillation measuring equipment the points for inversion conditions over grass were displaced above the dashed line. However, the data are consistent with the slope of the curve obtained for the data over snow.

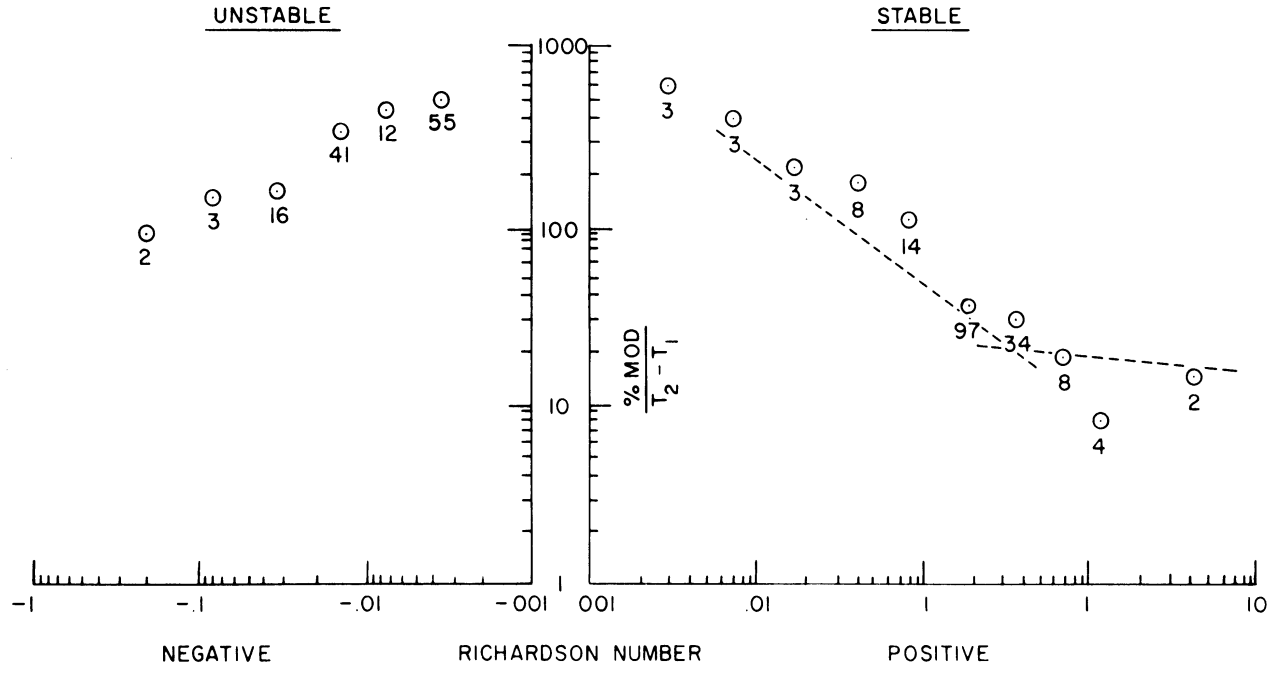

Figure 25. Per Cent Modulation Per Unit Temperature Difference Between 1 and 2 Meters vs. Richardson Number for Stable and Unstable Conditions over Grass

The relationship for negative Ri (unstable conditions) shows a decrease in P_m per unit temperature difference with increasing negative Ri. In the region of the curve with large negative $P_m/(T_2 - T_1)$ ratios and small negative Ri, for $P_m/(T_2 - T_1)$ to be about -500, for example, P_m was about 5 and $(T_2 - T_1)$ -0.01C. Such a condition of low scintillation intensity occurred shortly before sunset and after sunrise over a grass surface. In each case, scintillation became so low for a short time during the transition from inversion to lapse at sunrise and from lapse to inversion at sunset that P_m approached the noise level of the scintillation recording system. To compute Ri, the same temperature difference which was used in $P_m/(T_2 - T_1)$ was also used in the numerator of Ri and was divided by a vertical wind shear term squared. Other terms which entered into the computation of Ri such as average temperature, height, and gravity remained approximately constant.

For the region of the curve with smaller negative $P_m/(T_2 - T_1)$ ratios and larger negative Ri, for $P_m/(T_2 - T_1)$ to be about -100, for example, P_m was about 100 and $(T_2 - T_1)$ about -1C. Such a condition was common near midday over a grass surface with clear skies. In both the inversion and lapse conditions, the increase in absolute magnitude of Ri was caused by an average increase in $(T_2 - T_1)$ and a corresponding decrease in $V_2 - V_1$.

The variation of scintillation with respect to Ri and temperature differences at WRL and KFS was similar but the diurnal behavior was quite different. Over the grass surface at WRL, the diurnal pattern of vertical temperature gradients normally consisted of a daytime lapse and a nighttime inversion. This enabled the effects on scintillation of both positive and negative Ri and transition periods near sunrise and sunset to be studied. Over the snow cover at KFS, however, inversions of varying magnitude predominated both in daytime and at night, resulting in generally positive Ri.

In general, the relationships observed between P_m per unit temperature difference and Richardson number support the concept that scintillation should increase with an increase in wind speed, other variables remaining constant. Thus, the data shown in Figure 25 for Ri + 0.35 could be rearranged to give a relationship of the form

$$P_m = a\,(T_2 - T_1)^b \quad (u_2 - u_1)^{-c}$$

in which a, b, and c are positive numbers. It is to be noted that an increase in wind speed necessarily means an increase in $(u_2 - u_1)$. A relationship of this form is evident in Figure 10, Part I, which shows P_m as a function of both mean temperature difference and wind speed for inversion conditions over snow. More observations are required, however, to complete the analysis for lapse conditions.

5.2.3 Scintillation Per Cent Modulation and Path Length -- The increase of scintillation and other optical effects of turbulence with increasing length of optical path, L, were discussed in Part I. Results based on limited measurements indicated that the relationship $P_m \propto L^p$ in which p varied between 0.8 and 0.9 represented the increase of scintillation intensity between about 100 and 600 m. These findings agreed well with those of Gurvich, Tatarski, and Cvang (1958).

Additional measurements of this type were made during inversion conditions on two successive nights in 1962 (25 July, 1900-2200 EST and 26 July, 1950-2150 EST) over a uniform grass field. On 25 July, the inversion magnitude between 0.5 m and 2 m was +0.45C and the average wind speed at 1 meter was about 4 m/sec. On 26 July, the inversion was +1.1C and the wind speed at 1 meter was 180 cm/sec. The experiments were conducted with identical light sources at a height of one meter and at distances of 100, 300, 500 and 700 from the photometer.

The results of the experiment are shown in Fig. 26. Each point is the average of 21 individual observations for each path length. Average values of P_m increase logarithmically from about 5 at 100 m to 62 at 700 m according to the relationship $P_m \propto L^{1.3}$. The exponent 1.3 agrees well with the relationship obtained by Siedentopf and Wisshak (1948) for distances between L = 80 m and 400 m. However, it is larger than that obtained for earlier experiments at WRL.

The reason for the larger exponent obtained in the 1962 field experiments is believed to be that a different method was used to maintain a constant DC level (the voltage component of the photometer signal due to the average brightness of the light source) in recording the scintillation of the light sources at the various distances. The nearest light was much brighter and gave a higher DC level than the farthest, but it was desirable to keep the DC level approximately constant in the field experiments.

For the experiments discussed in Part I, a constant DC level was maintained by decreasing the aperture diameter of each nearer light source. The angular dimension as seen by the photometer also remained approximately constant. For the 1962 field experiments, in which smaller light source and photometer apertures were used, the method was to compensate for the increased brightness of each nearer source electrically at the photometer. The diameter of the light source aperture remained the same at each path length.

It is apparent that more experimentation and analysis are required to isolate the separate effects of DC level, the angular dimension of each light source as seen by the photometer, and the photometer aperture. All data obtained to date indicate, however, that the increase in scintillation (and, therefore, the deterioration in visual resolution) is approximately proportional to the length of the optical path.

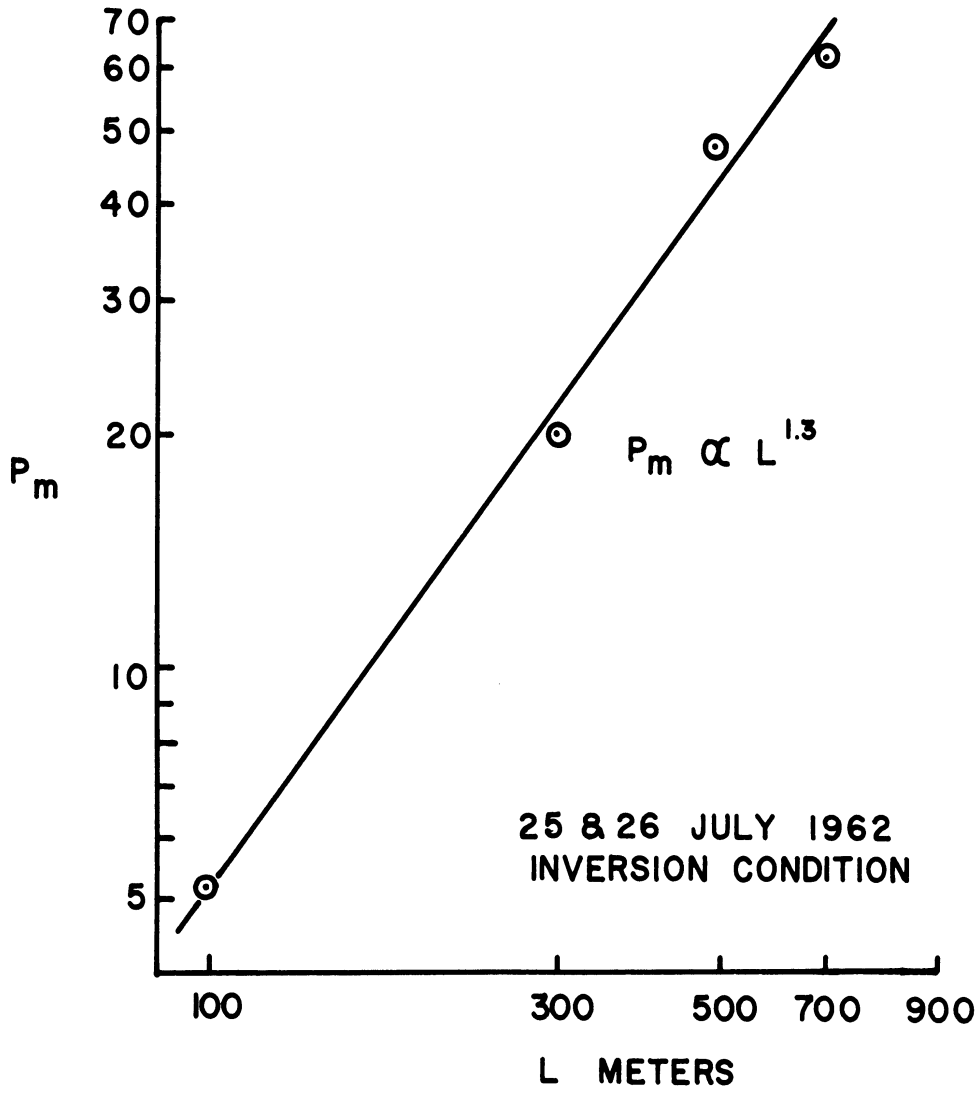

Figure 26. Per Cent Modulation vs. Path Length

6. SCINTILLATION POWER SPECTRA

6.1 Introduction

Spectral data for eight two-minute scintillation recordings were presented in Part I. The eight periods represented a wide range of resolution during inversion conditions over snow. It was reasoned that both the size and speed of inhomogeneities in the index of refraction would influence resolution and that insofar as these may be measured by spectral characteristics of scintillation, the latter should reveal important information for relating resolution to meteorological conditions. A spectral resolution factor was derived which appeared to have a close relationship to the limit of resolution for the eight periods analyzed.

In addition to the results obtained regarding the resolution aspect of the scintillation power spectra, preliminary findings regarding the meteorological aspects of the spectra were discussed qualitatively. Among these was a tendency for low frequencies to dominate for conditions with high positive Richardson numbers. After normalization to wind speed component perpendicular to the optical path, however, a correlation between stability and spectral characteristics was not apparent for the eight periods. The following sections discuss the analysis of additional spectra obtained over snow, grass-covered ground, and ice surfaces in relation to coincident meteorological conditions.

6.2 Equipment and Procedures

The equipment and procedures for recording and processing the magnetic tape recordings of scintillation frequency were similar to those of Parks (1960). Because they were described in Part I, only a brief summary is given here.

The selected periods of data were re-recorded on a Honeywell Model LAR 7490 Laboratory Analog Recorder/Reproducer. Recording tape speeds of 7 1/2 or 3 3/4 ips were used and playback from the tape loop was at 60 ips in all cases. Thus a frequency multiplication of 8 or 16, depending upon the speed of recording, was applied to the data.

The spectral density of discrete frequency bands was measured with a Hewlett-Packard Model 300A Harmonic Wave Analyzer. The bandwidth of the analyzer is about 10 cps, so that an effective bandwidth of 1.25 or 0.625 cps results after frequency multiplication. The lower frequency limit for analysis is determined by the bandwidth, and is 2.5 or 1.25 cps, respectively. The upper frequency limit of analysis capability is greater than the frequency having significant power in the scintillation spectra.

The output of the wave analyzer is the rms voltage contained in the particular frequency band of concern. Since this voltage exhibits some time

variation, it is recorded and manually averaged over the period of analysis. Although this method of reduction imposed some degree os subjective judgment into the analysis, repetitive analysis of a period of data indicated that the distribution of the spectral density curve was not likely to deviate by more than $\pm$ 3%.

6.3 Results

A list of analyzed spectra and coincident meteorological data important for their interpretation are given in Table VI. The spectra numbered 1 through 8 are those also discussed in Part I.

Eight additional (two to three-minute) periods of data obtained at the Keweenaw Field Station during February and March, 1960, were analyzed and are numbered from 9 through 16. Eighteen frequency recordings obtained over a grass surface at the Willow Run Field Station in 1962 were also analyzed. They include seven periods obtained during unstable thermal stratification and eleven periods obtained during stable conditions. They are labeled 1u through 7u and 1s through 11s, respectively, in Table VI. In addition, sixteen periods of data obtained over ice in 1963 were analyzed.

All data were adjusted to equivalent recorder gain prior to analysis. The spectra numbered 9 through 16 are shown in Fig. 27a and 27b and those numbered 1u through 5u and 1s through 6s are shown in Fig. 28a and 28b. The ordinate scale is power per unit frequency, $W_p(f)$. The subscript p, in accordance with Tatarski's (1961) notation, signifies that the data are averaged over the aperture area. The differences in ordinate scales in the figures should be noted. The spectra are shown in this form to prevent any misunderstanding as to the large variation in total power that is actually observed. The large variation is essentially measured by a corresponding variation in P_m as discussed previously.

One aim in the analysis of the scintillation power spectra is to determine the relative distribution of spectral density in relation to several influencing parameters. Therefore, the spectra are normalized to a common total area under the spectral density curve so that variations in the distribution of energy are directly comparable. The normalization is accomplished by applying the factor

$$\int_0^\infty W_p(f)\, df$$

for an arbitrary reference spectrum. For convenience, the spectra are graphed in units of $f\, W_p(f)$ vs. log f where f is frequency in cps and $W_p(f)$ is the normalized power spectral density. The same spectra shown in the previous figures are shown in normalized form in Figures 29a and 29b and 30 a and 30b. A grouping on the basis of thermal stability is indicated by the general

Table VI

SCINTILLATION POWER SPECTRAL AND METEOROLOGICAL DATA

Over Snow, KFS, 1960

Path Length: 543 m Photometer Aperture Dia.: 7.6 cm.
Path Height: 1.5 m Light Source Dia.: 12.7 cm

(Stable Thermal Stratification)

Period	Date	Time EST	$\bar{v}_{1.5m}$ cm/sec	$\bar{v}_n$ cm/sec	Ri	P_m	f_m cps	m
1	2/13	2131	137	69	0.185	62	10.6	0.266
2	3/8	0632	53	51	0.604	62	8.9	0.294
3	2/13	2054	94	60	0.164	39	9.6	0.275
4	2/23	2125	310	131	0.135	40	11.9	0.152
5	2/20	2017	72	46	3.770	28	6.9	0.252
6	2/12	2336	96	93	0.598	29	8.3	0.142
7	2/19	2217	462	264	0.012	11	26.9	0.169
8	2/24	2031	146	112	0.349	13	12.2	0.178
9	2/19	2216	494	283	0.007	11	27.9	0.163
10	2/19	2144	491	347	0.026	12	35.6	0.169
11	2/23	2124	267	121	0.118	43	11.9	0.162
12	2/24	2034	139	106	0.355	13	12.0	0.187
13	2/13	2122	138	69	0.676	48	12.6	0.301
14	2/27	2052	172	169	1.781	42	9.7	0.095
15	2/27	1858	110	108	4.087	38	8.2	0.128
16	2/13	2140	237	182	1.859	41	13.1	0.119

Over Grass, WRL, 1962

Path Length: 500 m Photometer Aperture Dia.: 5 cm
Path Height: 1 m Light Source Dia.: 5 cm

(Unstable Thermal Stratification)

Period	Date	Time EST	$\bar{v}_{1.0m}$ cm/sec	$\bar{v}_n$ cm/sec	Ri	P_m	f_m cps	m
1u	4/3	1555	389	376	-0.075	140	49.6	0.209
2u	4/10	1502	673	650	-0.013	126	73.5	0.179
3u	4/10	1530	614	610	-0.019	125	72.0	0.187
4u	4/10	1548	598	543	-0.015	112	64.4	0.187
5u	4/3	1756	222	218	-0.008	9	39.4	0.286
6u	8/15	1032	392	282	-0.068	90	34.9	0.248
7u	8/15	1055	430	319	-0.055	87	32.9	0.206

Table VI (Continued)

Over Grass, WRL, 1962

(Stable Thermal Stratification)

Period	Date	Time EST	$\bar{v}_{1.0m}$ cm/sec	$\bar{v}_n$ cm/sec	Ri	P_m	f_m cps	m
1s	4/3	1834	249	211	0.035	69	30.60	0.229
2s	4/3	1914	54	27	0.198	69	7.04	0.413
3s	4/3	1941	116	38	0.213	92	7.40	0.307
4s	4/3	2015	117	25	0.236	72	1.95	0.123
5s	4/3	2047	97	21	0.262	53	4.78	0.360
6s	4/3	2057	51	15	0.112	70	4.74	0.500
7s	7/25	2156	403	375	0.009	29	52.8	0.282
8s	7/25	2212	252	237	0.014	35	45.8	0.386
9s	7/26	2122	195	189	0.084	59	27.4	0.290
10s	7/26	2231	187	186	0.078	59	23.5	0.252
11s	7/26	2256	167	165	0.083	49	24.6	0.298

Over Snow-covered Ice, Whitmore Lake, 1963

Path Length: 500 m
Path Height: 1 m
Photometer Aperture Dia.: 5 cm
Light Source Dia.: 5 cm

Period	Date	Time EST	$\bar{v}_{1.0m}$ cm/sec	$\bar{v}_n$ cm/sec	Ri	P_m	f_m cps	m
1*	1/15	2038	201	83	-0.071	13	20.2	0.487
2*	1/17	1401	27	0	-0.151	5	4.4	-----
3*	1/17	1447	83	72	-0.015	6	16.7	0.464
4	1/23	1834	379	359	0.056	30	65.8	0.367
5	1/23	1914	451	325	0.058	27	53.2	0.327
6	1/31	1727	147	0	0.148	27	2.8	-----
7	1/31	1855	206	64.1	0.173	28	10.1	0.315
8	1/31	1933	110	106	0.461	19	16.8	0.317
9	1/31	2008	57	50	0.742	8	6.8	0.272
10	1/31	2010	28	25	0.288	6	5.9	0.472
11	1/31	2041	101	75	0.120	35	16.2	0.432
12	3/13	2235	67	31	0.102	4	19	0.123
13	3/13	2255	73	43	0.088	9	2.7	0.126
14	3/13	2321	57	52	0.222	7	3.4	0.131
15	3/14	1540	355	344	0.144	13	37.4	0.217
16	3/15	1434	192	174	0.026	7	48.7	0.559

*unstable stratification.

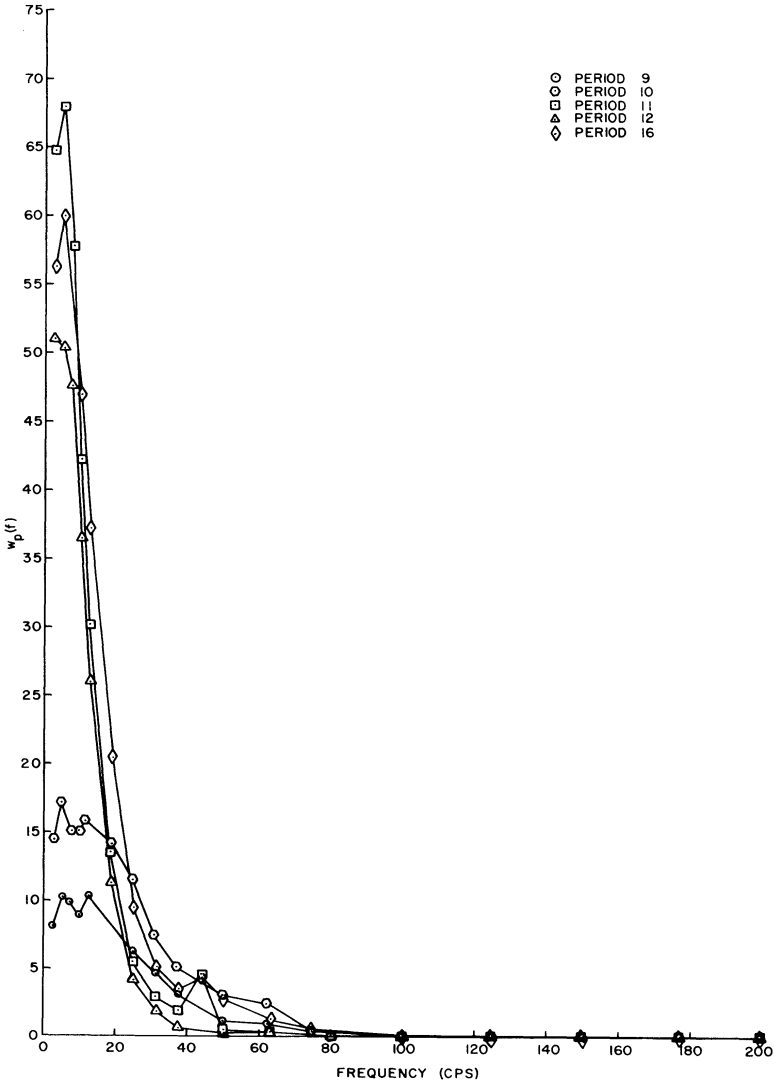

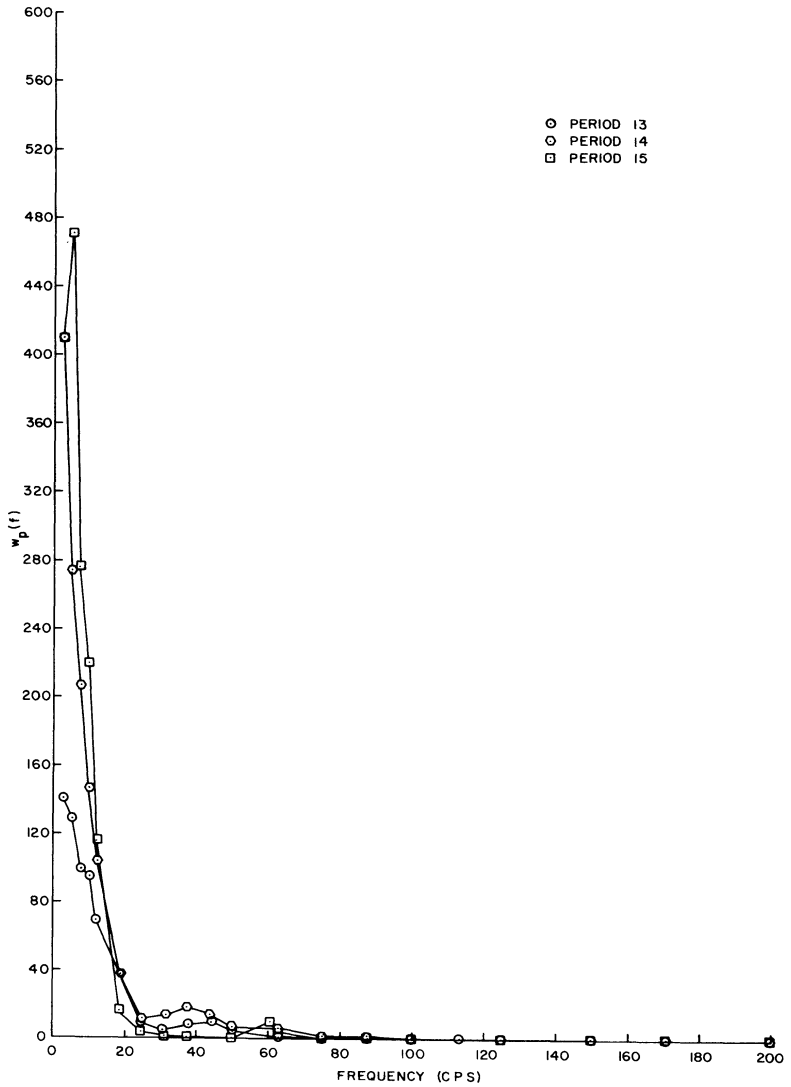

Figures 27a and 27b. Power Spectra of Scintillation for Stable Conditions over Snow

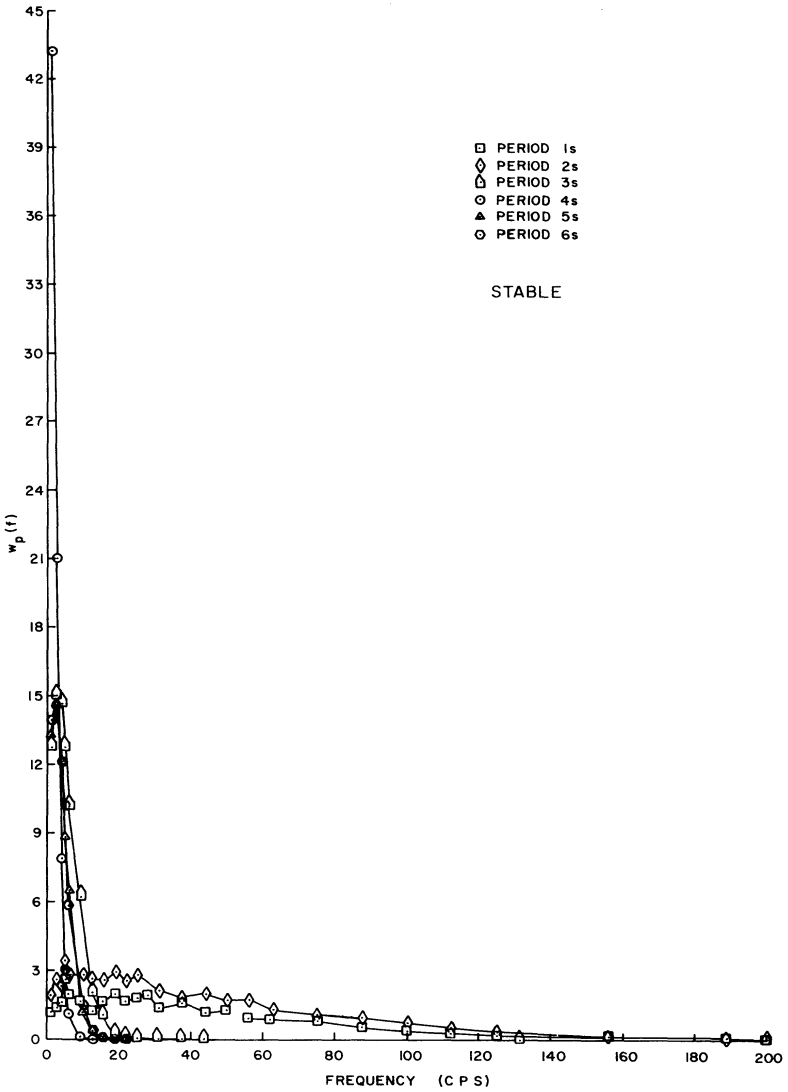

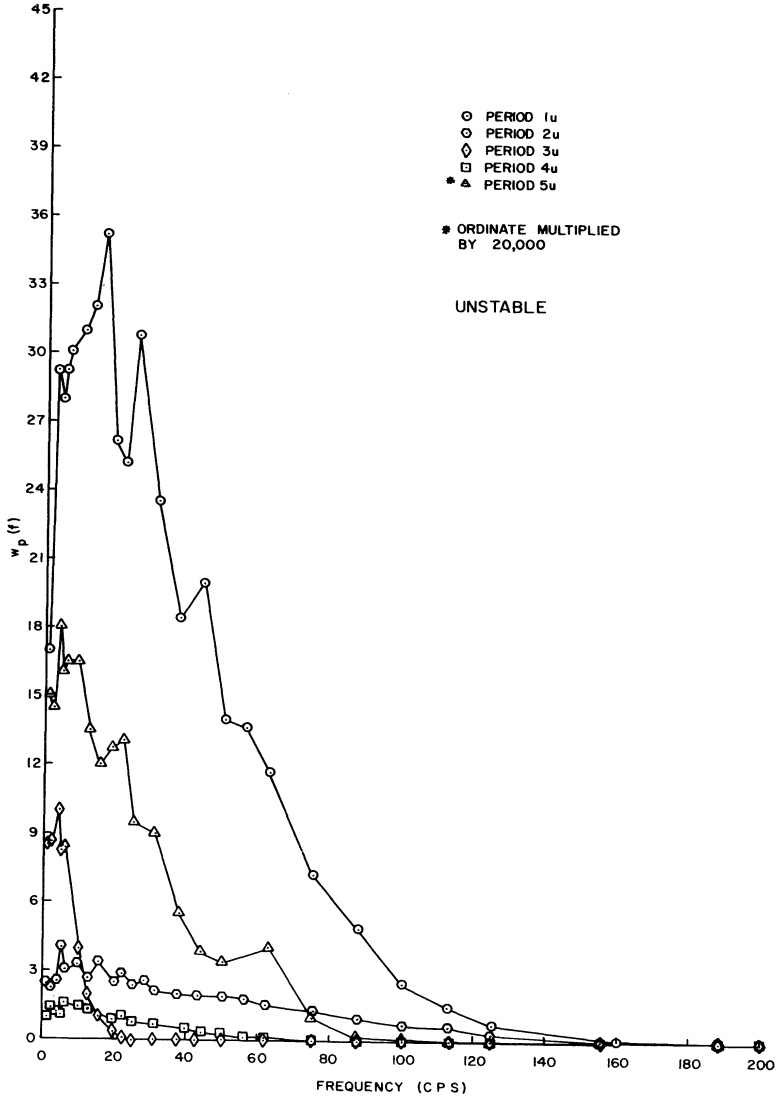

Figures 28a and 28b. Power Spectra of Scintillation for Stable and Unstable Conditions over a Grass Surface

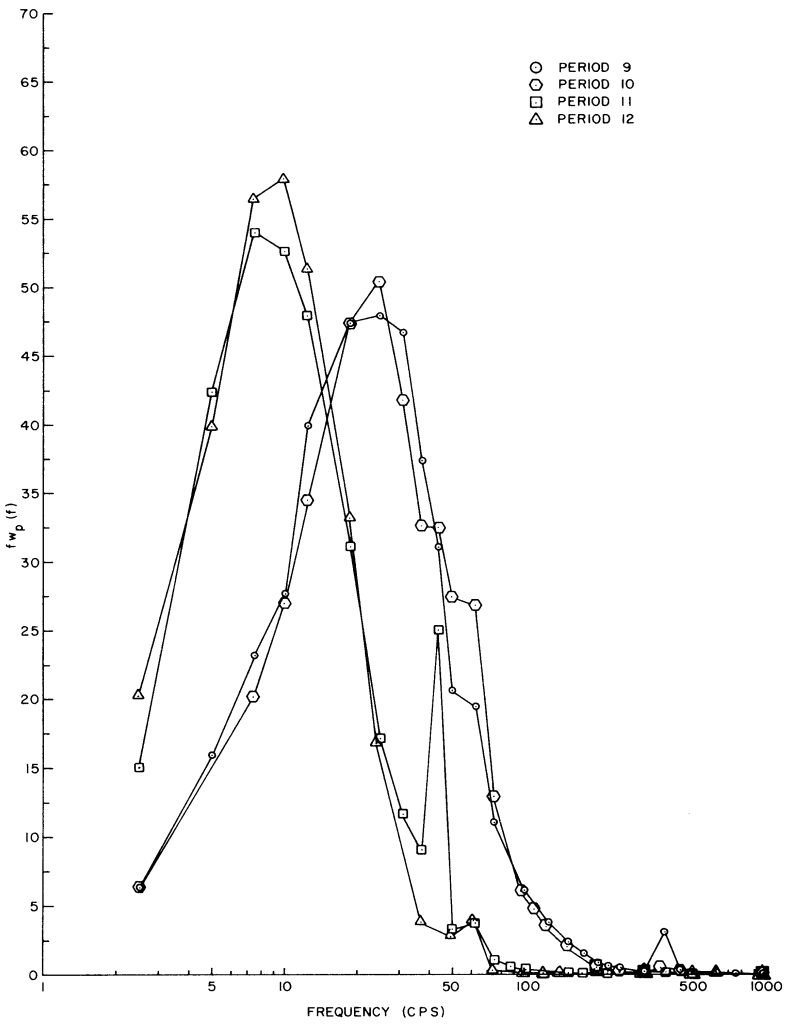

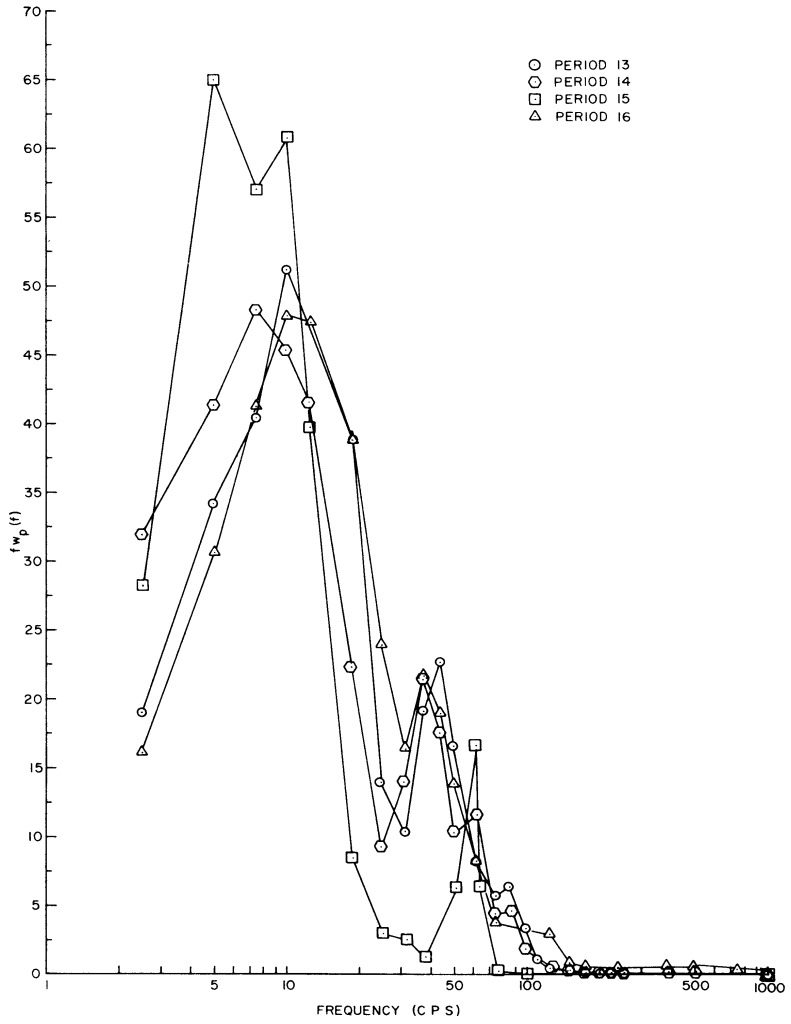

Figures 29a and 29b. Normalized Power Spectra of Scintillation for Stable Conditions over Snow (Power Per Logarithmic Frequency Increment)

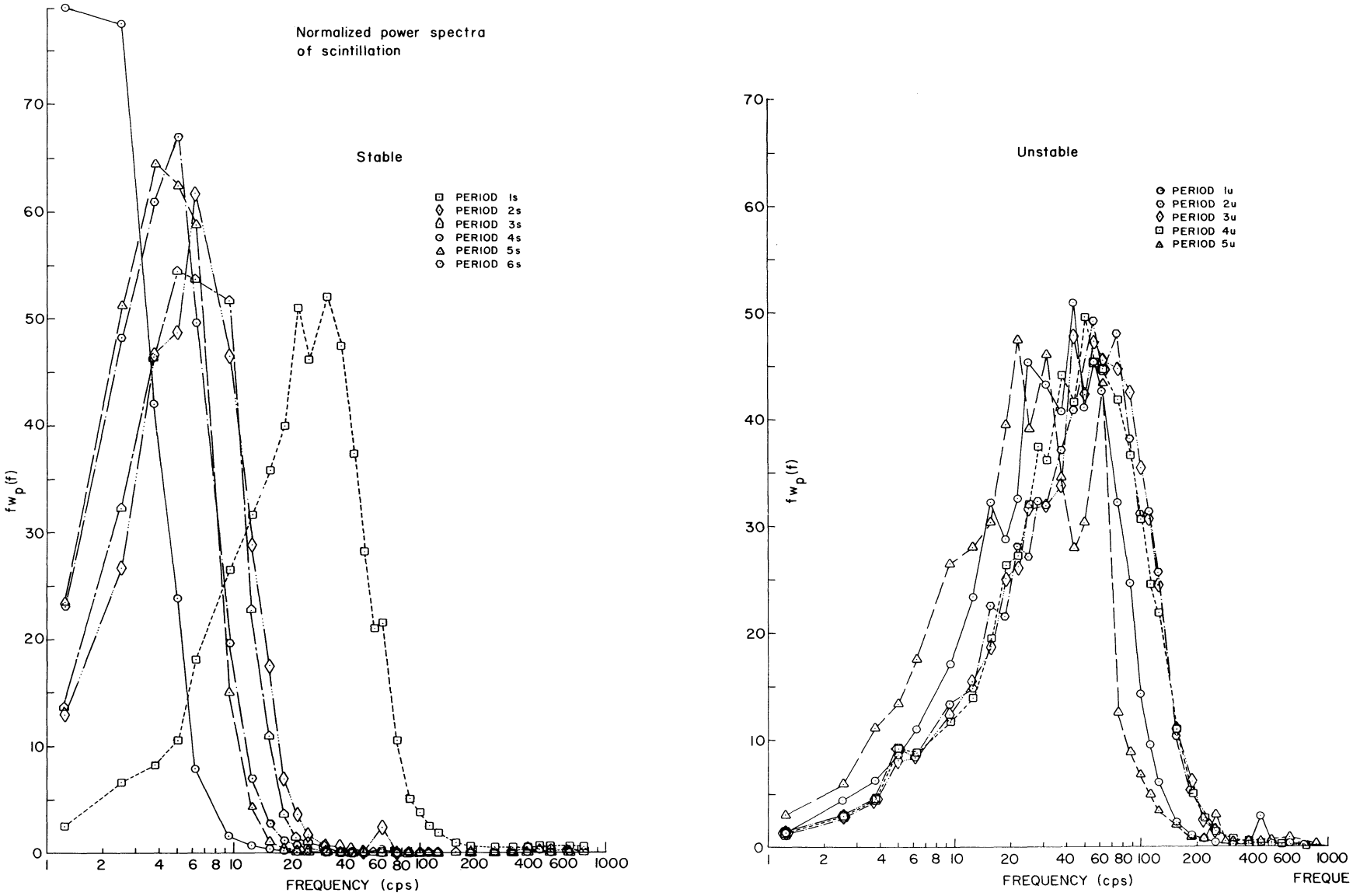

Figures 30a and 30b. Normalized Power Spectra of Scintillation for Stable and Unstable Conditions over a Grass Surface (Power Per Logarithmic Frequency Increment)

spectral distributions, but it will be shown that the distributions are instead primarily related to the wind speed as predicted by the theoretical development of Tatarski (1961).

6.4 Interpretation

With the assumption that refractive index inhomogeneities are "frozen in", i.e., do not change by a significant amount during advection across the photometer aperture, Tatarski (1961) developed an expression that described the power spectral density function of intensity fluctuations. He showed that the normalized spectral density function u(f) had the form

$$u(f) = \frac{f\, w(f)}{\int_0 w(f)df} = F\, \frac{f(\lambda L)^{1/2}}{\bar{V}_n}$$

where f = frequency of amplitude fluctuations (cps)
λ = wavelength of electromagnetic wave (cm)
L = path length of propagation (cm)
$\bar{V}_n$ = average wind speed normal to the path of propagation (cm/sec)

Thus, the normalized power spectra of scintillation should be expected to depend upon the wavelength of light, path length, and wind speed normal to the path.

It must be noted that the theoretical expression does not account for the effect of the photometer aperture. An "aperture smoothing" effect will occur if the aperture diameter exceeds the scale of the smallest inhomogeneities present in the intensity field. Tatarski's theory predicts that a reduction in the spectral density at the higher frequencies will occur when the aperture diameter exceeds $(\lambda L)^{1/2}$. Thus, according to the theory, a significant aperture smoothing effect may be present in the spectra presented in this report. No attempt was made to normalize the data for this factor.

The spectra may be compared conveniently in terms of the maximum value of $f\, w_p(f)$ when presented in the form of Figures 29 and 30. Following Tatarski (1961), the maximum, f_m, is defined as the average of two frequencies at which $f\, w_p(f)$ is one half the maximum measured value. The values of f_m have been computed for all analyzed spectra.

6.4.1 Power Spectra and Normal Wind Speed -- The relationship of f_m to $\bar{V}_n$ is shown in Fig. 31 for fifty spectra. The increase of f_m with increasing $\bar{V}_n$ is evident; that is, as the wind speed component normal to the optical path increases, the maximum normalized power shifts to higher frequencies. The regression equation for the relationship is $f_m = 2.52 + 0.12\, \bar{V}_n$.

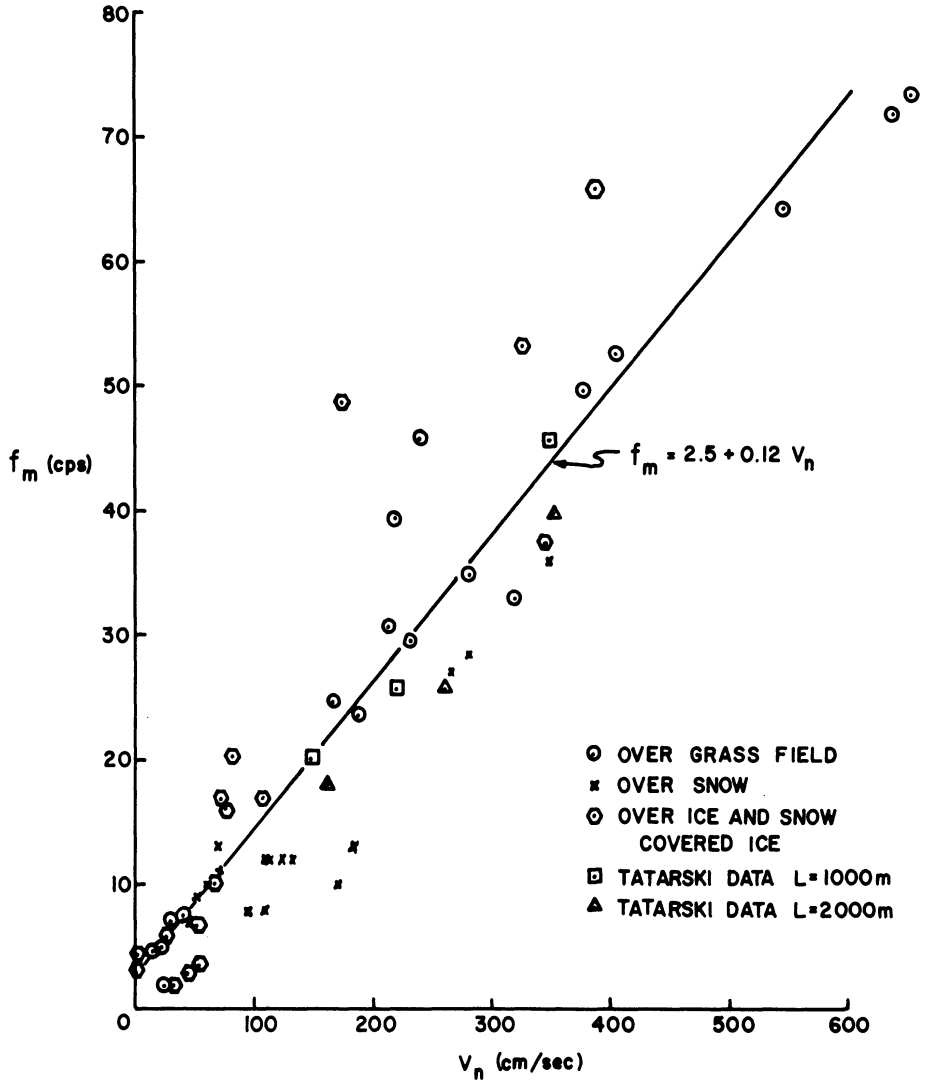

Figure 31. Power Spectra of Scintillation Maxima vs. Wind Speed Normal to Optical Path

The scatter of points around the regression line and the fact that $f_m = 2.52$ cps when $\bar{V}_n = 0$ could be partially due to the fact that both wind direction and profiles of wind speed were measured at only one point in the optical path and may not necessarily have represented conditions in the entire path. However, the scatter may represent a portion of the total variation of f_m not explained by the measurements of the normal wind speed. Other factors including the atmospheric stability may be important.

To eliminate the influence of normal wind speed, path length and wave length of light, the following parameter:

$$m = f_m \frac{(\lambda L)^{1/2}}{\overline{V}_n}$$

was defined. Tatarski's theoretical value for m, postulated for an infinitely small aperture, is 0.55. He found, however, an average experimental value of m = 0.32 for 80 spectra obtained with a 2 mm aperture. In the present analysis, m ranged from about 0.12 to 0.56 and had an average of 0.28 for the fifty spectra. The photometer aperture size used in the over-snow cases was 7.6 cm and a 5 cm aperture was used over grass and ice surfaces. It would be expected that m would shift to lower values for a larger aperture size, but this effect was not consistently observed. The variability of the parameter m, therefore, must also be attributed in part to errors in measurement of the normal wind speed or to other unmeasured variables.

6.4.2 Power Spectra and Path Length -- Tatarski supported his finding that the normalized frequency spectrum should depend only on the quantity $f(\lambda L)^{1/2}/\overline{V}_n$ by analyzing 80 spectra obtained at distances of 1000 and 2000 m. From these data, he obtained average values of m = 0.29 and 0.35 for $\lambda = 0.5 \times 10^{-4}$ cm for the two distances, respectively. Using the arithmetic average of these two values, he concluded that m = 0.32. If the wave length of $\lambda = 0.8 \times 10^{-4}$ cm and a path length L = 500 meters (from the present experiments) are substituted into Tatarski's expression, it becomes $f_m = 0.16\ \overline{V}_n$.

Measurements of scintillation for path lengths of 100, 300, 500 and 700 m were described in Section 5.3.2. A description of the coincident meteorological conditions was also included in that section. Power spectra were computed from data obtained at the different path lengths, and the resulting values of m were found to have a dependence on path length as indicated in Fig. 32. Shown also in Fig. 32 are Tatarski's experimental data from which he computed an average m equal to 0.32. It is evident that the latter data support the former to a certain extent. The suggested path length dependence of both sets of data, furthermore, is such that the quantity $f_m/\overline{V}_n$ remains essentially independent of path length. Thus, its average value was 0.14 in close agreement with the value of .12 given in the previous section. Both sets of experimental data tend not to support the theoretical result that scintillation power spectra depend on the quantity

$$f\ (\lambda L)^{1/2}/\overline{V}_n$$

In consideration of this conclusion, however, it must be noted that measurement error could contribute significantly to the observed discrepancy between theory and observation. Possible sampling error in measuring $\overline{V}_n$ has already been mentioned. A second factor that could explain, at least, the direction of departure of the observed from the theoretical value is the possible smoothing effect due to the finite size of the light sources. As noted in Section 5.2.3,

the light source size did not vary with path length so that the angular dimension as seen by the photometer decreased with path length. Although this factor was not considered in Tatarski's theoretical treatment, it would seem that it could be treated as a photometer aperture "smoothing" effect for the higher frequencies. Thus it could act to decrease f_m greater amounts for shorter path lengths. This effect has not been considered quantitatively. It appears that additional experimentation and theoretical development will be required to resolve the observed discrepancies.

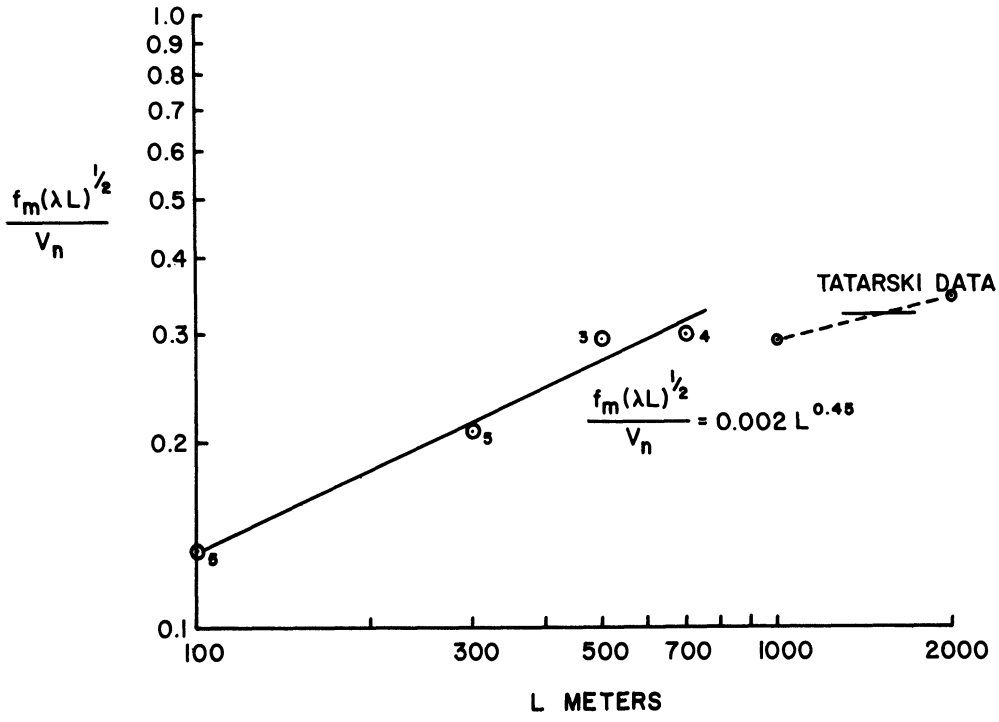

Figure 32. Normalized Power Spectra and Path Length

7. SUMMARY AND CONCLUSIONS

7.1 Visual Resolution for Stable Stratification over Snow

a) Resolution deteriorated systematically with increasing temperature difference. The smallest discernible slot size ranged from 0.34 inch with a temperature difference less than 1C between 50 and 400 cm to 0.76 inch with a temperature difference between 9 and 10C.

b) With clear or scattered sky conditions over snow at night, resolution deteriorated from about 0.38 to 0.72 inch as the 2 m wind speed increased from nearly calm to 5 mph and improved from 0.72 to 0.5 inch as the 2 m wind speed increased from about 5.0 to 8 mph.

c) With broken or overcast sky conditions resolution was much better (0.30 inch average) than during clear or scattered sky conditions and was nearly independent of wind speed.

7.2 Photographic Resolution

a) Photographic resolution, like visual resolution, deteriorated as scintillation increased. Although the photographic method had fewer disadvantages than the visual method, several problems remained unresolved.

   1) The method was not completely objective because an individual's judgment was necessary to determine the resolution limit either if the photographs were evaluated directly by him or if he evaluated a densitometer recorder trace.

   2) With the lens and resolution chart used, only six groups of lines separated the poorest from the best resolution. Either a more powerful lens or a chart with additional intermediate groups of lines would have provided more significant information.

7.3 Observations over Ice

a) Average scintillation intensity was low and resolution conditions were good during the observations over both clear ice and snow-covered ice. Not until a deeper snow cover (at least 10 cm) accumulated on the ice did conditions begin to approach those observed over land. Relatively small slot sizes of 0.24 inch or smaller were always discernible, contrasted to those 0.24 inch or larger which were discernible over the snow cover at KFS.

b) The relatively high conductive heat flux upward through clear ice, at times exceeding that of both soil and snow, is believed responsible for small average vertical temperature differences

above it and the resulting low scintillation intensity and good resolution conditions observed.

7.4 Willow Run Field Station Observations

a) The average effects of wind speed on scintillation for clear nighttime inversion conditions over a field covered with short grass were such that scintillation (1) increased rapidly and nearly linearly as wind speed increased from nearly calm to about 3 mph (2) rounded off through a peak at 4 mph and (3) decreased systematically at speeds greater than about 5 mph. At speeds greater than about 12 mph scintillation was at a minimum. With daytime lapse conditions and clear or scattered sky conditions scintillation intensity remained much higher at wind speeds of 10 mph or greater than with inversion conditions. It approached its lowest value above a speed of about 20 mph.

b) The relationships of scintillation per unit temperature difference to Richardson number over grass and stable and unstable conditions were similar. A decrease in the ratio with an increase in the absolute magnitude of Ri was observed in both stability conditions.

c) Findings (a) and (b) support the concept that P_m should increase with an increase in wind speed, other things remaining constant. In reality, vertical temperature gradients are inversely related to wind speed, but since temperature gradient information is not routinely available, the wind speed relationships provide useful information for estimating visual resolution and scintillation conditions from standard weather data.

d) Scintillation intensity increased systematically with increase in length of path between 100 and 700 m.

7.5 Power Spectra of Scintillation

a) A linear increase of the frequency of average maximum normalized power with an increase in the wind speed component normal to the optical path was observed.

b) A logarithmic increase of the quantity $fm\ (\lambda L)^{1/2}/V_n$ with path length was obtained for path lengths between 100 and 700 m. The quantity fm/V_n remained approximately constant with path length.

c) For engineering applications, the maximum spectral density of fluctuations of a light transmitted through a horizontal optical path will average below 20 cps.

REFERENCES

Boston University, 1957: An investigation of photographic techniques for the recording of missile flight, Boston Univ. Phys. Res. Lab., Final Report, 43-51.

Corps of Engineers, U. S. Army, 1957: "Effect of snowpack condition on runoff," Snow Hydrology, 285-318.

Liljequist, G. H., 1957b: Wind structure in the low layer, Norwegian-British-Swedish Antarctic Exped., Sci. Results, Vol. 2, Pt. 1C, 219-225.

Parks, J. K., 1960: "A comparison of power spectra of ocean waves obtained by an analog and a digital method," J. Geophys. Res., Vol. 65, No. 5, 1557-1563.

Portman, D. J., 1954: "Determination of the soil heat transfer at O'Neill, Nebraska," Publications in Climatology, Vol. III, No. (2), Johns Hopkins Univ. Lab. of Clim., 320-325.

_____ and E. Ryznar, 1961: Thermodynamic studies of a snow cover in Northern Michigan, SIPRE Res. Rep. 74, 73pp.

_____, F. C. Elder, E. Ryznar, and V. E. Noble, 1962: "Some optical properties of turbulence in stratified flow near the ground," J. Geophys. Res., Vol. 67, No. 8, 3223-3235.

_____, E. Ryznar, F. C. Elder and V. E. Noble, 1964: Visual resolution and optical scintillation over snow, ice and frozen ground, CRREL Res. Rep. No. 111, Pt. I.

Ratcliffe, E. H., 1962: "Thermal conductivity of ice: new data on the temperature coefficient," The Philosophical Mag., Vol. 7, No. 79,

Ryznar, E., 1963: "Visual resolution and optical scintillation in stable stratification over snow," J. App. Meteor., Vol. 2, No. 4, 526-530.

Siedentopf, von H., and F. Wisshak, 1948: Die Szintillation der Strahlung terrestrischer Lichtquellen und ihr Gang mit der Tageszeit, Optik, 3, 430-433.

Tatarskii, V. I., 1961: Wave Propagation in a Turbulent Medium, (translation by R. A. Silverman), New York, McGraw-Hill, 285pp.

Wimbush, M. H., 1961: Optical astronomical seeing: a review, Hawaii Inst. Geophys. Rep. No. 16, Sci. Rep. No. 1, (AD 265 402).